IEEE Access
Multidisciplinary | Rapid Review | Open Access Journal

Date of publication xxxx 00, 0000, date of current version xxxx 00, 0000.

Digital Object Identifier 10.1109/ACCESS.2017.Doi Number

Design, Implementation, and Optimization of Sliding Mode Controller for Automatic Voltage Regulator System

Murat Furat[1], Member, IEEE, Gökçen Gidemen Cücü[2]

[1]Electrical-Electronics Engineering Department, İskenderun Technical University, Hatay, 31200, Turkey
[2]Atlas Energy Thermal Power Plant, Hatay, 31200, Turkey
Corresponding author: Murat Furat (e-mail: murat.furat@iste.edu.tr).

ABSTRACT Academic studies on the Automatic Voltage Regulator (AVR) have focused on a linear mathematical model which lacks protective features. More accurate model of the AVR system includes protective features as described in IEEE standards. The AVR models without protective features, namely limiters, result in less accurate control performance since the outputs of real controllers are always bounded. In the present study, the controller outputs are limited between -0.9pu and 1.0pu, and the upper bound of exciter output is limited by 3.1pu with the direction of IEEE standards. The effect of limiters on the controller performance is investigated. Two controllers with a novel sliding surface function are proposed based on a mathematical model of the AVR (SMC_3) and its approximate reduced-order model (SMC_2). The proposed controllers having only two parameters are optimized with improved particle swarm optimization (PSO) algorithm. After optimization, the robustness of the controllers is compared with the results of various operating conditions identical to the previous studies. Nominal time constants of the AVR constituents are perturbed from -50% to 50%, and ±10% output disturbance is applied to the output. Although controller outputs and exciter output are limited, the overshoot is measured less than 0.1% at no-load conditions. The robustness of the controllers against parameter uncertainties is measured with an average overshoot at the output. Another superiority among the reported results in the literature is obtained from the proposed controllers, where the minimum average overshoots are measured. In addition, when ±10% load is applied to the output of the AVR, the proposed controllers generate accurate control inputs that reject the load disturbance successfully. Furthermore, the proposed controllers keep the output within the ±5% band if there is a monotonic change at the output. All the results show that the proposed controllers with the improved PSO have drawn the best performance from the perspective of time-domain specifications in comparison with the recently reported controllers.

INDEX TERMS Automatic voltage regulator, excitation limiter, particle swarm optimization, robust control, sliding mode control

I. INTRODUCTION

Electric power distribution networks continue to enlarge at a rapid rate due to the demand for different types of loads. The energy demand is provided continuously by a variety of power plants connected to the distribution network. In this network, the electrical energy flowing from the power plants to the loads should be regulated despite the load change on the distribution network. There are two important properties to be always regulated: operating frequency and operating voltage levels. The first one is directly related to the speed of the generator rotor while the operating voltage level changes with respect to the load on the power system or excitation of the synchronous generator. The frequency and voltage regulations are performed at the power plants. Both frequency and voltage levels are measured at the terminals of the generators, and proper controllers are used to ensuring their stability. Operation frequency is regulated with Load Frequency Controller (LFC), and an Automatic Voltage Regulator (AVR) is used to regulate the terminal voltage or reactive power of the synchronous generator.

The present study deals with the voltage regulation of the synchronous generators mounted in hydroelectric, thermoelectric, and wind power plants. On account of the

This article has been accepted for publication in a future issue of this journal, but has not been fully edited. Content may change prior to final publication. Citation information: DOI 10.1109/ACCESS.2022.3177621, IEEE Access

nonlinearities of the load in real distribution networks, fast and stable regulation is a big challenge for the AVR [1]. Therefore, the control strategies of the AVR systems are important for the reliability of power systems.

In the literature, plenty of the AVR controllers have been proposed based on proportional-integral-derivative (PID) controllers [1]. Due to the simple structure and well-known effects of each parameter on the output of the controlled system, the PID controller has been widely used in industrial applications [2]–[5]. Although different structures of PID controllers were proposed to control the AVR system in the literature, the main drawback of the conventional PID tuning methods, such as trial-and-error, Ziegler-Nichols, root-locus, is a lack of achieving good performance against uncertain system parameters and the load disturbance [5]–[7].

A conventional PID controller has been proposed for the AVR systems, and several metaheuristic algorithms were used to find optimum controller parameters [3], [4], [16]–[21], [8]–[15]. The controller performance in the related studies has been evaluated and compared with other studies. Since conventional PID controller is integer-order, FOPID controllers were also conducted with similar optimization algorithms [22]–[25]. Further improvements on FOPID have been recently proposed with variable-order [26]. It is obvious that the complexity of the FOPID controllers is more than integer-order PID since additional parameters are used [7], [27]. Another type of PID, the state-feedback PID, was also proposed [28], [29]. A robust 2DOF state-feedback PI-controller has been designed in [28] that eliminated steady-state error by the integral control. According to the results, 2DOF state-feedback PI-controller was better than 1DOF PI-controller. Further improvement on 2DOF state-feedback PI-controller was presented in [29] by using a dynamic weighted state-feedback approach. The flexibility of the proposed scheme against different system conditions was reported. A different controller, namely a robust state-feedback controller, was suggested for the AVR [30]. The suggested controller differs in that bounded system uncertainties and external disturbances were considered in the controller's design. In order to overcome the uncertainty problem of the AVR system, a non-fragile PID controller tuned with a genetic algorithm [21] and a model predictive controller optimized by AOA [7] were proposed.

Although PID controllers have been studied intensely, different control schemes can be found in the literature. A robust controller based on H∞ and μ-analysis was suggested for robust stability against parametric and structured uncertainties and disturbances [2]. A fractional-order model reference adaptive control scheme was proposed with the genetic algorithm [31]. In [32], an imperialist competitive algorithm was used to tune the neural network predictive controller for the AVR. In a recent study, an emotional deep learning programming controller (EDLPC) for the AVR has been proposed which contained an emotional deep neural network (EDNN) structure and an artificial emotional Q-learning algorithm.

The number of the parameters to be tuned increases when the complexity of the controllers increases. As the advances in computational systems have increased in the last few decades, metaheuristic optimization algorithms have become more prevalent in optimization problems. The general principle of these algorithms was to minimize or maximize the selected objective function so that the terminal voltage level was kept more accurate. The optimum magnitude of each controller parameter was investigated among a specified value of candidates, which are generally chosen randomly in a bounded search space. Then, the optimum value was iteratively searched using the optimization algorithm's principle without complex mathematical derivations. In order to obtain a fast response with good transient-state, ABC [20], AOA [7], CS [15], ECSA [25], EOA [16], FSA [17], IKA [1], IWO [23], PSO [8], [33], SCA [24], and hybrid algorithms [9], [22] can be found in the literature. Each optimization algorithm has own superiority to the others to find the optimal solution [34].

Generally, the search spaces for conventional PID controller parameters have been defined between 0.2 and 2.0 [13]. Different types of objective functions have been formulated in order to find the optimal controller parameters. Error-based performance indices, time domain specifications, and frequency domain parameters have been used frequently. Commonly preferred performance indices are ISE, IAE, ITSE, and ITAE, time-domain specifications are maximum peak (M_o), overshoot ($OS\%$), steady-state error (e_{ss}), settling time (t_s), and rising time (t_r) obtained from the step response data and frequency domain parameters are phase margin (PM) and gain margin (GM). In the literature, the objective functions have been formulated not only with one of the performance indices [22], [29], [32], but also the combined functions are defined with appropriate weighting constants [6]–[8], [11], [15], [21], [35]. A single function may not be efficient for the optimization of all controller parameters, while it is a difficult task to determine the weighting constants of combined objective functions [11]. A comparative study on the combined performance indices was evaluated with PID controller tuning by a tree-seed algorithm [14].

The performance of the controllers and the success of the selected optimization algorithms were evaluated against parameter uncertainties and voltage regulation of generator terminals [2]. The fluctuations in the terminal voltage, even small in magnitude, may cause severe damage to the connected electrical devices on the distribution network [35]. Therefore, the performance of the proposed controllers for the AVR has also been evaluated with respect to the transient and steady-state step responses and load disturbance rejection capability [25].

This article has been accepted for publication in a future issue of this journal, but has not been fully edited. Content may change prior to final publication. Citation information: DOI 10.1109/ACCESS.2022.3177621, IEEE Access

NOMENCLATURE

ABC: Artificial Bee Colony Algorithm
ACO-NM: Hybrid Ant Colony Optimization and Nelder Mead
AOA: Arithmetic Optimization Algorithm
AVR: Automatic Voltage Regulator
BA: Bat Algorithm
BBO: Biogeography-based Optimization
CAS: Chaotic Ant Swarm Optimization
CS: Cuckoo Search Algorithm
CSA: Crow Search Algorithm
DA: Dragonfly Algorithm
DEA: Differential Evolution Algorithm
ECSA: Enhanced Crow Search Algorithm
EOA: Equilibrium Optimizer Algorithm
FLC: Fuzzy Logic Controller
FOPID: Fractional Order Proportional-Integral-Derivative Controller
FP+FI+FD: Fuzzy P + Fuzzy I + Fuzzy D Controller
FPA: Flower Pollination Algorithm
FSA: Future Search Algorithm
GA: Genetic Algorithm
GA-BF: Hybrid Genetic Algorithm and Bacterial Foraging
GOA: Grasshopper Optimization Algorithm
GWO: Gray Wolf Algorithm
HGAPSO: Hybrid Genetic Algorithm and Particle Swarm Optimization
IAE: Integral Absolute Error
IKA: Improved Kidney-inspired Algorithm
ISE: Integral Squared Error
ITAE: Integral Time Multiplied Absolute Error
ITSE: Integral Time Multiplied Squared Error
IWO: Invasive Weed Optimization
KHA: Krill Herd Algorithm
LFC: Load Frequency Controller
LUS: Local Unimodal Sampling Algorithm
MFO: Moth-Flame Algorithm
MOEO: Multi-objective Extremal Optimization
MOL: Many Optimizing Liaisons Algorithm
NSGA: Non-dominated Genetic Algorithm
OEL: Overexcitation Limiter
OVL: Overvoltage Limiters
PID: Proportional-integral-derivative
PSA: Pattern Search Algorithm
PSO: Particle Swarm Optimization
PSOGSA: Hybrid Particle Swarm Optimization and Gravitational Search Algorithm
SA: Simulated Annealing
SCA: Sine Cosine Algorithm
SCL: Stator Current Limiter
SFS: Stochastic Fractal Search
SISO: Single Input Single Output
SMC: Sliding Mode Control
SOS: Symbiotic Organism Search
SSA: Salp Search Algorithm
TLBO: Teaching-learning based Optimization
TSA: Tree Seed Algorithm
UAV: Unmanned Aerial Vehicle
UEL: Underexcitation Limiter
VSA: Vortex Search Algorithm
WCA: Water Cycle Algorithm
WOA: Whale Optimization Algorithm
WWO: Water Wave Optimization

A. DISCUSSION ON THE PREVIOUS STUDIES

The studies in the literature on the control of the AVR can be investigated with the following highlights:

- Proposed controllers
- Proposed parameter optimization algorithms
- Superiority comparison (other controllers or optimization algorithms)

Among the controllers recommended for the AVR, there are a significant number of conventional PID and PID-based controllers. In Table I, selected studies on the AVR are summarized concerning the highlights above.

As seen in Table I, the studies on the control of the AVR can be classified into two groups. In the first group, the aim of the studies with conventional PID is to present how superior the proposed optimization algorithm is to the other algorithms. The only difference in these studies is the optimization algorithm, as stated in [2]. A good comparison can be found in [25]. In the remaining studies, new controllers are proposed with different optimization algorithms. Further critical comments on the optimization algorithms used for PID tuning with transient-state response specifications were given in [16].

Remark 1: In the light of the interest in metaheuristic optimization algorithms, the rising question is to understand how an optimization algorithm is suitable for the control of the AVR. It is evident that no algorithm fits all the optimization problems [3]. Each optimization algorithm has superiority over each other in different aspects, as stated in "no free lunch theorems" [36], [37]. New optimization algorithms are being developed to overcome the constraints of existing ones.

The metaheuristic optimization algorithms in Table I give satisfactory results if the following parameters are appropriately selected:

- Sufficiently large and correct search space for each controller parameter
- Sufficient number of population individuals
- Sufficient number of iterations
- Correct algorithm gains
- Adequate number of free runs
- The proper objective function(s) to be minimized or maximized

Furthermore, the optimization algorithms can be improved according to the controller [25]. Besides, the whole performance of the proposed controllers depends on the robustness of the controller against parameter uncertainties and disturbances [2].

Remark 2: The efforts on the control of the AVR have been performed with a linear model of the AVR which includes an amplifier, an exciter, a sensor, and a synchronous generator [29]. The control input of the proposed controllers was applied directly to the AVR without any limiters. However, the control input must be limited against overexcitation and underexcitation of the synchronous generator. Overexcitation causes the excessive current in the field circuit of the generator which results in heating and underexcitation causes the generator to operate it outside of the underexcited region. The excitation limiters, which are overexcitation limiters (OEL) and underexcitation limiters (UEL) prevent the generator from operating out of the

This article has been accepted for publication in a future issue of this journal, but has not been fully edited. Content may change prior to final publication. Citation information: DOI 10.1109/ACCESS.2022.3177621, IEEE Access

allowable operating region [38], [39]. In addition to these limiters, overvoltage limiters (OVL), stator current limiters (SCL), and volts-per-hertz limiters are used in modern excitation systems [40], [41]. These limiters make the linear model of the AVR system non-linear [39], [42].

Since the practical application of the controllers proposed for the AVR is difficult, an effective way is to use suitable mathematical models which represent the actual performance of the excitation system of a synchronous generator. In this context, the models presented in IEEE standards can be used as the most appropriate mathematical models for academic studies [40], [41]. The protection accessories of the models presented in *IEEE Std 421.5-2016 Recommended Practice for Excitation System Models for Power System Stability Studies* [40] and *IEEE Std 421.2-2014 Guide for Identification, Testing, and Evaluation of the Dynamic Performance of Excitation Control Systems* [41] are the excitation limiters which are generally neglected in the literature [43]. The simulation results, obtained from the linear model of the AVR without including OEL and UEL in the excitation systems, may not be valid for real applications [40], [41]. In practice, the range of excitation current is between 1.6-3.0pu. According to [43], the excitation current out of the limits is difficult to realize because of the magnetic saturation. Therefore, in the present study, the limits were defined in the direction of IEEE [44], which reflects the real exciter features in the simulation results.

Remark 3: An important barrier to the configuration of an optimization algorithm is the number of controller parameters to be tuned. As the number of controller parameters is increased, defining sufficiently large and correct search space for each parameter will be difficult. There are three parameters to be tuned for the conventional PID controller. However, up to 7 parameters were reported for different structures of PID controllers proposed for the single input single output the AVR [24]. It is usually preferable to have a single controller with the fewest adjustable parameters to accomplish superior terminal voltage regulation [45].

TABLE I
LITERATURE REVIEW OF THE PID CONTROLLERS AND CORRESPONDING OPTIMIZATION ALGORITHMS PROPOSED FOR THE AVR

Ref #	Proposed Controller	Optimization Algorithm	Superiority Comparison
[8]	Conventional PID Controller $C(s) = k_p + \frac{k_i}{s} + k_d s$	PSO	GA
[9]		Taguchi combined GA	GA, PSO
[10]		LUS	PSO, ABC, DEA
[11]		PSO with multi-objective Pareto front solution	Different error-based performance criteria
[12]		PSOGSA	Ziegler-Nichols, PSO, MOL
[3]		SOS	ABC, MOL, BBO
[13]		SFS	ABC, MOL, LUS, WCO, BBO
[4]		WWO	BA, CSA, FPA, PSO, SCA
[14]		TSA	IKA, LUS, ABC, PSO, DEA, PSA, BBO
[15]		CS	PSO, GA, CAS
[16]		EOA	PSO, ACO-NM,GA-BF
[17]		FSA	ABC, TLBO, MOEO, NSGA
[18]		Canceling zeros by poles	---
[25]		ECSA	Results of 21 different PID-based AVR studies
[19]		WCA	GA, SA, DA, KHA, ABC, LUS, MOL, TLBO
[20]		Comparative analysis of PSO, DEA and ABC	
[46]	PID with Filtered Derivative Action $C(s) = k_p + \frac{k_i}{s} + k_d s\left(\frac{1}{s(1/N)T+1}\right)$	TLBO	Sugeno FLC, Mamdani FLC, GA, PSO, LUS, ABC, DE
[1]	PID with First-order Filter $C(s) = k_p + \frac{k_i}{s} + \frac{k_d s}{T_f s+1}$	IKA	PSO, DE, ABC, LUS, PSA, BBO, GOA
[22]	FP+FI+FD Controller	HGAPSO	Conventional PID, Fuzzy PID
[23]	FOPID	IWO	Conventional PID
[24]	FOPID, FOPID with Integer Filter, PID with Integer Filter, PID with Fractional Filter	SCA	Conventional PID and FOPID optimized with SA, CAS, MOEO, PSO, GA, BBO, ABC
[35]	FOPID	JOA	Conventional PID optimized with DE, PSO, ABC, BBO, GOA, PSA, IKA, LUS, FOPID optimized with SSA
[28]	2DOF State Feedback PID	PSO	PSO tuned 1DOF PI, PSO tuned 2DOF PI
[29]	2DOF Dynamically Weighted State Feedback PID	VSA, SCA, GWO, WOA, SSA, MFO, WCA	PSO

This article has been accepted for publication in a future issue of this journal, but has not been fully edited. Content may change prior to final publication. Citation information: DOI 10.1109/ACCESS.2022.3177621, IEEE Access

B. CONTRIBUTION OF THE PRESENT STUDY

In the previous section, common drawbacks of the recent studies were discussed. Generally, the evaluations were performed for the robustness of the proposed controllers against load disturbance rejection performance and parameter uncertainties. Adaptive control, self-tuning control, variable structure control, and direct feedback linearization (DFL) techniques were used to give dynamic stability to power systems over a wide range of operating points [47]. Therefore, conventional sliding mode control (SMC) is well fitted for the AVR control problem. Contrary to the previous studies, a novel SMC strategy is followed in this study. Tuning of the controller parameters is performed by using improved particle swarm optimization (PSO) algorithm.

The contributions of the present study can be outlined as follows:

- Model-based sliding mode controllers are designed for the AVR systems with a novel sliding surface rule.
- A straightforward design procedure of the controllers is provided step by step.
- The limiters are introduced at the output of the controller and the exciter in accordance with the direction of IEEE standards.
- The stability of the proposed controller is guaranteed in the sense of Lyapunov stability theorem subjected to the lumped uncertainty and output disturbances.
- Traditional PSO is improved for the proposed controllers so that a customized objective function is defined for each controller parameter.
- Only two controller parameters are optimized in the AVR system.
- Overshoot at the output is restricted in the objective functions of the improved PSO.
- Various operating conditions identical to previous studies are evaluated for comparison.
- The effect of the limiters on the performance of the controllers is compared with the linear AVR.
- Enhancement of the improved PSO is compared with traditional PSO.

The remaining of the study is organized as follows. In the following section, the AVR model with the limiters is introduced. In section 3, detailed design procedures of the proposed sliding mode controllers are derived. Different design requirements are explained for SMC in this section. The mathematical basis of the improved PSO for the proposed controllers is given in section 4. In section 5, detailed comparisons are performed between conventional AVR and AVR with limiters, traditional and improved PSO, SMC_2 and SMC_3. All the results are compared graphically and statistically with the related studies in the literature. Finally, all the results are summarized in the last section.

II. DESCRIPTION OF LINEAR AVR MODEL WITH THE LIMITERS

In previous studies, the authors preferred the state-variable methodology for the model of the AVR [48]. A conventional AVR mainly consists of four constituents: an amplifier, an exciter, a sensor, and a synchronous generator [2], [29], [49], as seen in Fig. 1. The mathematical model of each AVR constituent is simplified with the first-order transfer function, ignoring saturation or any nonlinear state [13]. In order to make the comparison in a fair and informative manner, the same mathematical model of the AVR is considered in the present study. Typical transfer functions of each AVR constituent are constructed by a time constant and a gain. The transfer functions and parameter ranges are given in Table II [24], [35], [49], [50].

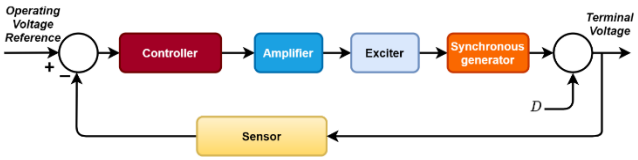

FIGURE 1. Conventional AVR model

TABLE II
FUNDAMENTAL CONSTITUENTS OF AN AVR WITH LINEARIZED TRANSFER FUNCTIONS AND CORRESPONDING PARAMETER RANGES

AVR constituents	Transfer functions	Selected gains and time constants	Parameter Ranges
Amplifier	$G_a(s) = K_a / (1+\tau_a s)$	$G_a(s) = 10/(1+0.1s)$	$10 \le K_a \le 40,\ 0.02s \le \tau_a \le 0.1s$
Exciter	$G_e(s) = K_e / (1+\tau_e s)$	$G_e(s) = 1/(1+0.4s)$	$1 \le K_e \le 10,\ 0.1s \le \tau_e \le 0.4s$
Generator	$G_g(s) = K_g / (1+\tau_g s)$	$G_g(s) = 1/(1+s)$	$0.7 \le K_g \le 1.0,\ 1.0s \le \tau_g \le 2.0s$
Sensor	$G_s(s) = K_s / (1+\tau_s s)$	$G_s(s) = 1/(1+0.01s)$	$0.9 \le K_s \le 1.1,\ 0.001s \le \tau_s \le 0.06s$

It is possible to come across many studies in the literature that do not limit the control inputs. Nevertheless limiting the control input significantly affects the closed-loop performance of the controllers in real systems [51]. Unlike the cited studies, the limiters are introduced for the controller input and the exciter to prevent the generator from overexcitation and underexcitation. These limiters result in nonlinear characteristics [39], [42]. Because of this reason, the transient performance of the AVR system is crucially affected. The detailed structures of limiters of the AVR

This article has been accepted for publication in a future issue of this journal, but has not been fully edited. Content may change prior to final publication. Citation information: DOI 10.1109/ACCESS.2022.3177621, IEEE Access

system were presented in [40]. A saturation function is used to simplify the limiters that limit the control input and exciter output between their maximum and minimum values. The tracking of the control input was only given in [7], [11], [31], [32].

Different types of excitation system models were introduced in IEEE standards [40]. Among the excitation system models, the maximum and minimum control input defined for the DC1C excitation system model is considered for the present study. The output of the proposed sliding mode controller is limited between -0.9pu and 1.0pu and the saturation factor of the exciter is defined as 3.1pu. The schematic diagram of the AVR with the proposed SMC and connected to a distribution network is depicted in Fig. 2. In the present study, the load frequency controller is assumed to work stable.

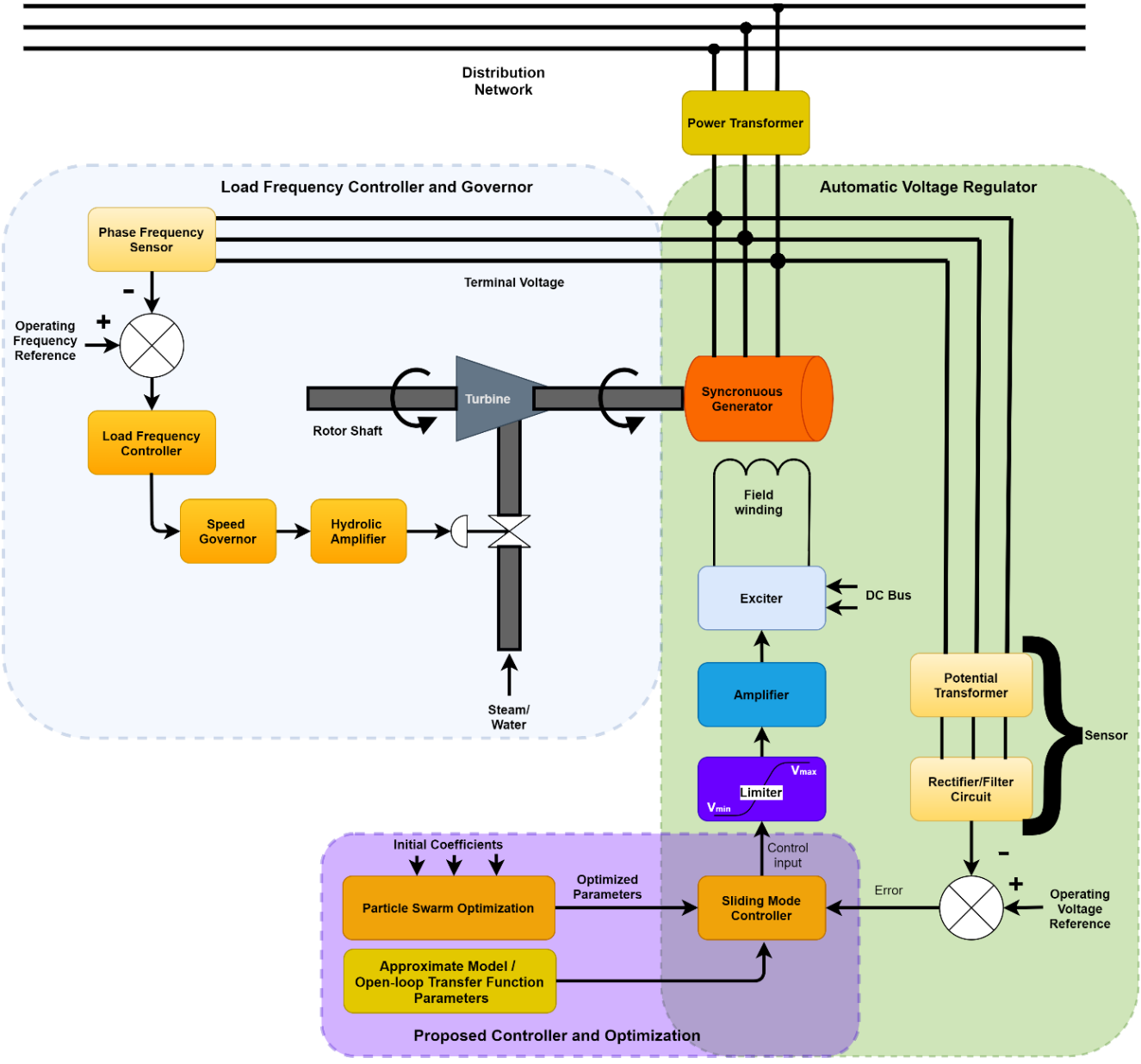

FIGURE 2. **The schematic diagram for synchronous machine and proposed excitation control system**

III. PROPOSED SMC DESIGN PROCEDURE

One of the effective control schemes to obtain an accurate control input in the presence of model uncertainties and output disturbances is SMC. The SMC schemes can be classified as first-order SMC schemes which are also known as conventional SMC and high-order SMC schemes. In the conventional SMC schemes, the control input is obtained using a straightforward solution with the approximate model of the system [52]. This solution was also successfully applied with second-order SMC [53]. Another types of SMC schemes are second-order algorithms, namely, drift, twisting, super-twisting and sub-optimal [54].

Among these algorithms, super-twisting control is more prevalent in the literature [55]–[58].

The SMC schemes can be either model-based or non-model-based. The non-model-based schemes have been widely used in practical applications at a price of limited performance. On the other hand, an approximate mathematical model is adequate to design the model-based SMC. Besides, the model-based SMC schemes provide robust control input that rejects matched uncertainties and output disturbances. In particular, their systematic design procedure with an approximate system model has made the SMC attractive since it was first introduced in the literature [53], [59]. Furthermore, fast dynamic response, high accuracy, stability, and simplicity of implementation are the other SMC features in industrial applications [60]. In addition, a sliding-mode based variable structure control was proposed for a nuclear reactor power system with LSA for obtaining an efficient controller against output disturbances and parameter uncertainties [61].

Because of the reasons mentioned above, the model-based SMC is preferred to control the AVR. The design procedure of the proposed controllers is as follows:

Step 1: Exact mathematical model or approximate model of the system is obtained.

Step 2: A sliding surface function is defined with the system states. It is generally a function of tracking error and its derivatives.

Step 3: The equivalent control law is investigated in the derivatives of the sliding surface function.

Step 4: Ideal sliding mode is obtained.

Step 5: The switching control law is decided in the sense of stability.

Step 6: The control input is obtained by summing the equivalent and the switching control laws.

A. GENERALIZED SYSTEM DESCRIPTION

Consider an n[th]-order, uncertain, SISO, linear system with parameter uncertainties and output disturbances of the form:

$$s^n Y(s) = \sum_0^{n-1} \left[-\left(a_i \pm \tilde{a}_i\right) s^i \right] Y(s) + bU(s) \pm D(s) \quad (1)$$

where

$Y(s)$: System output,

$U(s)$: Control input,

a : Nominal system parameter,

$\tilde{a}$: Uncertainty of the system parameter a

n : Order of the system

$D(s)$: Output disturbance

Rearranging the system given in (1), one has:

$$\begin{aligned} s^n Y(s) = &-\left(a_{n-1}s^{n-1} + a_{n-2}s^{n-2} + \ldots + a_0\right) Y(s) \\ &+ bU(s) + D(s,\tilde{a}) \end{aligned} \quad (2)$$

where $D(s,\tilde{a})$ is lumped uncertainties and output disturbances of the system, which can be expressed as:

$$D(s,\tilde{a}) = \left(\pm\tilde{a}_{n-1}s^{n-1} \pm \tilde{a}_{n-2}s^{n-2} \pm \ldots \pm \tilde{a}_0\right) Y(s) \pm D(s) \quad (3)$$

$D(s,\tilde{a})$ is bounded, $\left|D(s,\tilde{a})\right| < D_{\max}$, $D_{\max} \in R^+$ and $D_{\max}$ can be expressed as:

$$D_{\max} = \sum_0^{n-1} \left|\tilde{a}_i s^i Y(s)\right| + \left|D(s)\right| \quad (4)$$

Remark 4: In practice, bounded uncertainties and disturbances are allowed to impact a system within the operating region. If the total impact of the uncertainties and disturbances pushes the system out of the operating region, the protective devices activate to protect the system. Therefore, we need to assume an uncertain bounded term in the model of the AVR system that impacts when the controllers are active in the operating region. In the literature, this approach was used in the mathematical model of electromechanical systems [52], [53], multirotor UAV controlled with SMC [62], and higher-order models of synchronous generators under external disturbances [63]. In addition, bounded external disturbance and system uncertainties were considered in the design of a robust state-feedback controller recently [30].

B. PROPOSED SLIDING SURFACE DESIGN RULE

In the conventional SMC, it is well-known that the construction of the sliding surface is the most critical step of the design procedure. In the present study, a new rule is proposed for the sliding surface. The proposed rule is suitable to design SMC with a relative degree of 1 for n[th]-order uncertain linear systems, as follows:

$$\sigma_n(s) = \sum_0^{n-1} k_i s^i E(s) \quad (5)$$

where k_i is the sliding surface parameter, $k_i > 0$.

The tracking error is described as:

$$E(s) = R(s) - Y(s) \quad (6)$$

where $R(s)$ is the set point and $Y(s)$ is the output in Laplace form.

The control input is derived from the sum of the two control laws:

$$u_n = u_{eqn} + u_{swn} \quad (7)$$

where u_{eqn} and u_{swn} are equivalent and switching control laws for an n[th]-order system, respectively.

The switching control law enforces the tracking error towards the origin of the sliding surface. The control law is designed as relay-like control to ensure a fast dynamic response against output disturbances. Therefore, it is also known as the discontinuous control law. The switching control law is directly related to the transient-state performance and disturbance rejection ability of the controller. When the tracking error reaches to the origin of the sliding surface, the equivalent control law keeps the system at the origin where both error and its derivative is zero. Hence, it is also known as the continuous control law,

This article has been accepted for publication in a future issue of this journal, but has not been fully edited. Content may change prior to final publication. Citation information: DOI 10.1109/ACCESS.2022.3177621, IEEE Access

which provides the performance of the controller at the steady-state.

It is obvious that the modern systems are too complex to predict the actual behavior of the system with the uncertainties in the parameters caused by aging of mechanical equipment, thermal stress and other unpredictable reasons in the operating process. Therefore, in the academic studies, simplified mathematical models of AVR constituents have been used. When considering the all the system with uncertain parameters, we may need to represent the system with an approximate model obtained by open-loop response. Since, the proposed SMC schemes are capable of designing with the approximate model, we designed two types of SMC based on the degree of the system model.

In the present study, the open-loop unit step response of the AVR is used in the design procedure of the proposed sliding mode controller. Two different controllers are designed for $n=2$ and $n=3$. The stability of both controllers is guaranteed in the sense of Lyapunov stability theorem. The third-order model is obtained directly from the open-loop model of the AVR, while the second-order model is approximated from the unit step response of the open-loop AVR model.

C. DESIGN OF SMC WITH SECOND-ORDER APPROXIMATED MODEL OF AVR (SMC2)

A second-order, uncertain, linear system with respect to (1) is as follows:

$$\begin{aligned} s^2Y(s) = &-\left[\left(a_1 \pm \tilde{a}_1\right)s + \left(a_0 \pm \tilde{a}_0\right)\right]Y(s) \\ &+ bU(s) + D(s) \end{aligned} \tag{8}$$

Rearranging (8), one has:

$$s^2Y(s) = -a_1sY(s) - a_0Y(s) + bU(s) + D(s,\tilde{a}) \tag{9}$$

Then, the transfer function of the system with nominal parameters, $D(s,\tilde{a})=0$, in time domain is as follows:

$$\ddot{y}(t) = -a_1\dot{y}(t) - a_0y(t) + bu(t) \tag{10}$$

The sliding surface for $n=2$ obtained from the proposed rule given in (5):

$$\sigma_2(s) = k_0E(s) + k_1sE(s) \tag{11}$$

Taking inverse Laplace transform of (11) results in:

$$\sigma_2(t) = k_0e(t) + k_1\dot{e}(t) \tag{12}$$

where $e(t) = r(t) - y(t)$, $r(t)$ is set point, and $y(t)$ is the system output.

In order to obtain continuous control law u_{eq}, the derivative of $\sigma(t)$ is taken until the control input appears. In the proposed rule in (6), it appears in the first-order derivative of (12):

$$\dot{\sigma}_2(t) = k_0\dot{e}(t) + k_1\ddot{e}(t) \tag{13}$$

where $\ddot{e}(t) = \ddot{r}(t) - \ddot{y}(t)$. Substituting $\ddot{e}(t)$ and (10) into (13) yields:

$$\begin{aligned} \dot{\sigma}_2(t) &= k_0\dot{e}(t) + k_1\left[\ddot{r}(t) - \ddot{y}(t)\right] \\ \dot{\sigma}_2(t) &= k_0\dot{e}(t) + k_1\left[\ddot{r}(t) + a_1\dot{y}(t) + a_0y(t) - bu(t)\right] \end{aligned} \tag{14}$$

u_{eq2} can be found by $\dot{\sigma}_2(t)=0$:

$$u_{eq2} = \frac{1}{k_1b}\left[k_0\dot{e}(t) + k_1\left(\ddot{r}(t) + a_1\dot{y}(t) + a_0y(t)\right)\right] \tag{15}$$

The equivalent control law with lumped uncertainty is as follows:

$$\tilde{u}_{eq2} = u_{eq2} - b^{-1}D(t,\tilde{a}) \tag{16}$$

Then, the control input becomes:

$$\tilde{u}_2 = \tilde{u}_{eq2} + u_{sw2} \tag{17}$$

The ideal sliding mode can be derived by substituting (17) into (14) as follows:

$$\begin{aligned} \dot{\sigma}_2(t) &= k_0\dot{e}(t) + k_1\left[\ddot{r}(t) + a_1\dot{y}(t) + a_0y(t) - b\left(\tilde{u}_{eq2} + u_{sw2}\right)\right] \\ \dot{\sigma}_2(t) &= k_0\dot{e}(t) + k_1\left[\ddot{r}(t) + a_1\dot{y}(t) + a_0y(t) - bu_{sw2}\right] \\ &\quad -k_1b\left\{\frac{1}{k_1b}\left[k_0\dot{e}(t) + k_1\left(\ddot{r}(t) + a_1\dot{y}(t) + a_0y(t)\right)\right]\right. \\ &\quad \left. -b^{-1}D(t,\tilde{a})\right\} \end{aligned}$$

After simplifications, the ideal sliding mode is found as:

$$\dot{\sigma}_2(t) = -k_1bu_{sw2} + k_1D(t,\tilde{a}) \tag{18}$$

Lyapunov stability theorem is generally preferred in the literature to guarantee the asymptotic stability of the conventional SMC schemes [52], [53], [61], [64]. $\sigma(t)=0$ must be satisfied for SMC of relative degree 1. Therefore, a positive definite Lyapunov function is selected as follows:

$$V(t) = 0.5\sigma_2^2(t) \tag{19}$$

Substituting (18) into the first time derivative of (19) gives:

$$\begin{aligned} \dot{V}(t) &= \sigma_2(t)\dot{\sigma}_2(t) \\ \dot{V}(t) &= \sigma_2(t)\left(-k_1bu_{sw2} + k_1D(t,\tilde{a})\right) \\ \dot{V}(t) &= -\sigma_2(t)k_1bu_{sw2} + k_1\sigma_2(t)D(t,\tilde{a}) \end{aligned} \tag{20}$$

At this step, the switching control law is selected as:

$$\begin{aligned} u_{sw2} &= k_{sw2}\,\mathrm{sgn}\left(\sigma_2(t)\right) \\ u_{sw2} &= k_{sw2}\left|\sigma_2(t)\right| / \sigma_2(t) \end{aligned} \tag{21}$$

where k_{sw2} is switching gain, $k_{sw2} > 0$.

Substituting (21) into (20), one obtains:

$$\begin{aligned} \dot{V}(t) &= -\sigma_2(t)k_1bk_{sw2}\left|\sigma_2(t)\right| / \sigma_2(t) + k_1\sigma_2(t)D(t,\tilde{a}) \\ \dot{V}(t) &= -k_1bk_{sw2}\left|\sigma_2(t)\right| + k_1\sigma_2(t)D(t,\tilde{a}) \\ \dot{V}(t) &\le -k_1bk_{sw2}\left|\sigma_2(t)\right| + k_1\left|\sigma_2(t)\right|D(t,\tilde{a}) \\ \dot{V}(t) &= \left|\sigma_2(t)\right|\left(-k_1bk_{sw2} + k_1D(t,\tilde{a})\right) \\ \dot{V}(t) &\le \left|\sigma_2(t)\right|\left(-k_1bk_{sw2} + k_1D_{\max}\right) \\ \dot{V}(t) &= -\left|\sigma(t)\right|k_1\left(bk_{sw2} - D_{\max}\right) \\ \dot{V}(t)\Big|_{k_{sw2} > \frac{D_{\max}}{b}} &< 0 \end{aligned} \tag{22}$$

This article has been accepted for publication in a future issue of this journal, but has not been fully edited. Content may change prior to final publication. Citation information: DOI 10.1109/ACCESS.2022.3177621, IEEE Access

If the switching gain is selected as $k_{sw2} > \frac{D_{\max}}{b}$, then the proposed controller is stable.

D. CHATTERING REDUCTION

Conventional SMC schemes suffer from chattering, which is a high-frequency oscillation of switching control law. As stated in [52], if the gain of switching control is set large, faster convergence is obtained with chattering in the steady-state. On the other hand, the convergence will be slow if the magnitude of the switching gain is small. In the literature, smooth switching is preferred [65].

A control input having chattering may lead to infeasibility for the real AVR applications. In the literature, fractional approximation [66], saturation [67], [68] or hyperbolic tangent (tanh) [64], [69], [70] functions were preferred for smoothing of control inputs of conventional SMC schemes whose relative degrees are generally one or two. Besides, drift, twisting, super-twisting, and sub-optimal sliding mode controllers were developed to overcome chattering without using a model of the controlled system [54]. For more smooth control input, tanh-based super-twisting controller was also proposed recently [56]. As a result, *tanh* is frequently the preferred function for smoothing control input of SMC.

In the present study, to get smooth transitions in the switching control, *tanh* function with a smoothing constant is preferred instead of sign function as follows [53]:

$$u_{sw2} = k_{sw2} \tanh\left(k_{sf}\sigma_2(t)\right) \tag{23}$$

where k_{sw2} is the switching gain, $k_{sw2} > 0$, k_{sf} is the smoothing constant, $0 < k_{sf} < 1$.

Finally, the control input in (17) is found as:

$$\begin{aligned}\tilde{u}_2 = \frac{1}{k_1 b}\left[k_0\dot{e}(t) + k_1\left(\dddot{r}(t) + a_1\dot{y}(t) + a_0 y(t)\right)\right] \\ - b^{-1}D(t,\tilde{a}) + k_{sw2}\tanh\left(k_{sf}\sigma_2(t)\right)\end{aligned} \tag{24}$$

Although the switching control is smoothed with (23), when a sudden disturbance has occurred at the output, the switching rule behaves as a sign function until the error converges to zero. At that time, the limiter, introduced at the output of the controller, limits the calculated control input. Then, the actual control input of SMC_2 applied to the exciter becomes as in the following rule:

$$\tilde{u}_2^{\text{limited}} = \begin{cases} u_{\max} & \text{if } \tilde{u}_2 > u_{\max} \\ \tilde{u}_2 & \text{if } u_{\min} \geq \tilde{u}_2 \geq u_{\max} \\ u_{\min} & \text{if } \tilde{u}_2 < u_{\min} \end{cases} \tag{25}$$

The final control input, between the minimum and the maximum limits, changes smoothly.

E. DESIGN OF SMC WITH THIRD-ORDER OPEN-LOOP MODEL OF AVR (SMC_3)

A third-order model of the AVR can be expressed with model uncertainties and output disturbances by using (1) as follows:

$$\begin{aligned}s^3Y(s) = -\left[\left(a_2 \pm \tilde{a}_2\right)s^2 + \left(a_1 \pm \tilde{a}_1\right)s + \left(a_0 \pm \tilde{a}_0\right)\right]Y(s) \\ + bU(s) + D(s)\end{aligned} \tag{26}$$

Following the descriptions in (2)-(4), one has bounded lumped uncertainties, $D_{\max}$, where $|D(s,\tilde{a})| < D_{\max}$, $D_{\max} \in R^+$.

Then, the third-order model with the nominal parameters, $D(s,\tilde{a}) = 0$, in time-domain is as follows:

$$\dddot{y}(t) = -a_2\ddot{y}(t) - a_1\dot{y}(t) - a_0 y(t) + bu(t) \tag{27}$$

In this step, the sliding function can be constructed for the third-order system using the proposed rule in (5):

$$\sigma_3(s) = k_0E(s) + k_1sE(s) + k_2s^2E(s) \tag{28}$$

Time-domain representation of (27) is obtained by inverse Laplace transforming as follows:

$$\sigma_3(t) = k_0e(t) + k_1\dot{e}(t) + k_2\ddot{e}(t) \tag{29}$$

The first-order derivative of the sliding surface in (28) is taken to get u_{eq3}:

$$\dot{\sigma}_3(t) = k_0\dot{e}(t) + k_1\ddot{e}(t) + k_2\dddot{e}(t) \tag{30}$$

where $\dddot{e}(t) = \dddot{r}(t) - \dddot{y}(t)$. Substituting $\dddot{e}(t)$ and (27) into (30), one has:

$$\begin{aligned}\dot{\sigma}_3(t) = k_0\dot{e}(t) + k_1\ddot{e}(t) \\ + k_2\left(\dddot{r}(t) + a_2\ddot{y}(t) + a_1\dot{y}(t) + a_0 y(t) - bu(t)\right)\end{aligned} \tag{31}$$

From (30), u_{eq3} can be found by $\dot{\sigma}_3(t) = 0$:

$$\begin{aligned}u_{eq3} = \frac{1}{k_2 b}\left[k_0\dot{e}(t) + k_1\ddot{e}(t)\right. \\ \left. + k_2\left(\dddot{r}(t) + a_2\ddot{y}(t) + a_1\dot{y}(t) + a_0 y(t)\right)\right]\end{aligned} \tag{32}$$

The equivalent control law with the lumped uncertainty becomes $\tilde{u}_{eq3} = u_{eq3} - b^{-1}D(t,\tilde{a})$. In order to derive the ideal sliding mode, the procedure in section 3.3 is followed. After simplifications, the ideal sliding mode is found as:

$$\dot{\sigma}_3(t) = -k_2 b u_{sw3} + k_2 D(t,\tilde{a}) \tag{33}$$

Because of the systematic design procedure and the proposed rule for sliding surfaces, it is easy to guarantee asymptotic stability by using Lyapunov theorem. Choosing (19) and following the solutions, one can have the same switching control law given in (21). Then, in order to

This article has been accepted for publication in a future issue of this journal, but has not been fully edited. Content may change prior to final publication. Citation information: DOI 10.1109/ACCESS.2022.3177621, IEEE Access

overcome the chattering issue, the smooth control law in (23) can be used. At the end of the derivation of control input for the third-order model, the following expression with the smooth switching control law is obtained:

$$\tilde{u}_3 = \frac{1}{k_2 b}\Big[k_0\dot{e}(t) + k_1\ddot{e}(t) + k_2\left(\dddot{r}(t) + a_2\ddot{y}(t) + a_1\dot{y}(t) + a_0 y(t)\right)\Big] - b^{-1}D(t,\tilde{a}) + k_{sw3}\tanh\left(k_{sf}\sigma_3(t)\right) \quad (34)$$

As described in (25), the actual control input of SMC_3 is limited as follows:

$$\tilde{u}_3^{\text{limited}} = \begin{cases} u_{\max} & \text{if } \tilde{u}_3 > u_{\max} \\ \tilde{u}_3 & \text{if } u_{\min} \geq \tilde{u}_3 \geq u_{\max} \\ u_{\min} & \text{if } \tilde{u}_3 < u_{\min} \end{cases} \quad (35)$$

The overall block diagram of the proposed SMC scheme is depicted in Fig. 3

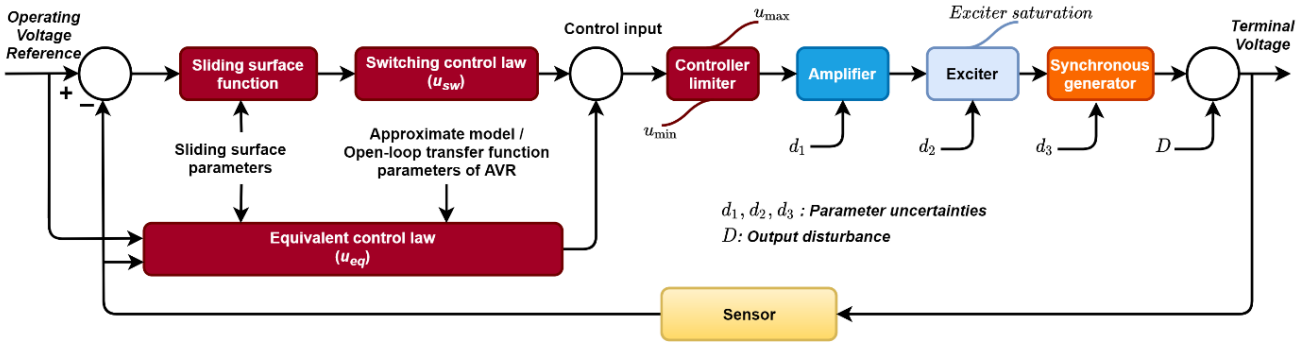

FIGURE 3. **Proposed SMC scheme**

F. ANALYSIS OF CONTROLLER PARAMETERS

In the present study, two controllers are proposed for the AVR based on the sliding surface function in (5). The proposed sliding surface function includes tracking error and its derivatives. The coefficients of the function can be simplified concerning the open-loop transfer function gain of the AVR as follows:

$$k_i = K^{-i}k_0 \quad (36)$$

where $i = 1, 2, ..., n-1$, n is the order of the open-loop AVR model and K is the open-loop transfer function gain.

In addition, the smoothing factor in the switching control, k_{sf}, can be selected as constant to reduce the chattering. By using the simplifications above, there are two controller parameters to be optimized, namely k_0 and k_{sw}.

In the real system optimization, trial-and-error method generally has been preferred by the expert staff for achieving the desired controller performance. In addition, Ziegler-Nichols and root locus tuning methods were also suggested for optimal controller parameters. As stated in [5], [6], [61], these methods are far from reducing the effects of parameter uncertainties and load disturbance. Therefore, metaheuristic search algorithms have been frequently preferred to find optimal controller parameters in the literature. In the present study, the PSO algorithm was improved for the proposed SMC schemes.

IV. IMPROVED PSO FOR THE PROPOSED SMC SCHEMES

The popular metaheuristic algorithms, generally called bio-inspired algorithms, are based on the behaviors of animals in nature. In addition to animal behaviors, laws of chemical and physical reactions are also used to develop new optimization algorithms. Systematic classification of these algorithms can be found in [71]. The most popular algorithms used in optimization problems do not need complex mathematical derivations to characterize the swarming behavior of animals in nature. This is one of the reasons for these algorithms being popular in order to find optimum solutions for complex problems. The optimal solution is searched in the pre-defined search space subjected to the constraints of the problem.

Among these algorithms, PSO is one of the most active optimization algorithms which is capable of finding the optimum solution. It was first proposed in [72] based on the behavior of fish or birds in nature. Because of its satisfying performance and its simple structure with an affinity toward manufacturing, PSO has been used in different applications.

PSO algorithm, by nature, optimizes the particles with respect to the positions of local and global best particles. Among the particles, the worst particle of the population is also moving in the direction of previous local and global best particles. Although current technology provides high-speed computations for simulations, it does not fit real systems. An applicable optimization algorithm to the real systems needs to be designed so that the algorithm is able to find optimum parameters with a minimum number of experiments. For this purpose, a novel strategy is improved in the proposed PSO algorithm.

In the present study, traditional PSO is improved for the optimization of proposed SMC parameters. The principle of the improved PSO is based on shrinking the initial search space concerning the worst particle position. At the end of each iteration, the worst particle is exchanged for a new particle randomly selected from the updated search space.

This property of the proposed PSO increases the probability of finding a global optimum in that space. Another property of the improved algorithm is using a customized objective function for each controller parameter. Instead of using a single or combined objective function, customized objective functions concerning the effect of controller parameters are introduced to get better optimization. Overshoot at the output of the generator terminal is not desired. Therefore, the particles that result in overshoot are labeled as the worst particles with a decay coefficient. In the literature, the worst particles were rarely used in PSO [73]–[75].

A. MATHEMATICAL DESCRIPTION OF THE IMPROVED PSO

Let X denote a multidimensional search space represented as:

$$X = \begin{bmatrix} k_{1\min} & k_{1\max} \\ k_{2\min} & k_{2\max} \\ \vdots & \vdots \\ k_{m\min} & k_{m\max} \end{bmatrix} \tag{37}$$

where $k_{i\min}$ and $k_{i\max}$ are lower and upper bound of the search spaces, $k_{i\min}, k_{i\max} \in R^{+}$ and $i = 1,2,3,\ldots m$.

Let k_i^j is a random variable distributed uniformly in upper and lower bounds of the corresponding search space, $k_i^j \in \left[k_{i\min}, k_{i\max}\right]$ and $j = 1,2,3,\ldots,n$. The set of all random variables can be expressed in the following way:

$$K = \begin{bmatrix} k_1^1 & k_1^2 & k_1^3 & \cdots & k_1^n \\ k_2^1 & k_2^2 & k_2^3 & \cdots & k_2^n \\ \vdots & \vdots & \vdots & \cdots & \vdots \\ k_m^1 & k_m^2 & k_m^3 & \cdots & k_m^n \end{bmatrix} \tag{38}$$

where n is the number of variables uniformly distributed in each search space. The probability density of finding optimum parameters in the search spaces are in the following:

$$f_{k_i}(X) = \frac{1}{\Delta X} \tag{39}$$

where

$$\Delta X = \begin{bmatrix} k_{1\max} - k_{1\min} \\ k_{2\max} - k_{2\min} \\ \vdots \\ k_{m\max} - k_{m\min} \end{bmatrix} \tag{40}$$

Consider a swarm-based optimization of a controller having m parameters. In order to measure the performance of the controller by using the variables in (37) as the parameters of the controller, a set of customized objective functions are described as follows:

$$P = \begin{cases} p_1\left(k_i^j\right) \text{ for } i = 1 \\ p_2\left(k_i^j\right) \text{ for } i = 2 \\ \vdots \\ p_m\left(k_i^j\right) \text{ for } i = m \end{cases} \tag{41}$$

In the present study, at each iteration of the optimization, m parameters are simultaneously assigned to the controller for n times. At the end of each iteration, the best and the worst objective function is determined as:

$$\left.\begin{aligned} P_{best} &= \min(P) \\ P_{worst} &= \max(P) \end{aligned}\right\} \tag{42}$$

Generally, large magnitudes of the controller parameters cause instability at the output. On the other hand, small magnitudes of the controller parameters do not provide satisfactory performance. The parameters that give best output are, in fact, the parameters that make up the best combination. In order to achieve good convergence to the global optimum parameters, the initial search spaces are shrunk at the end of each iteration with respect to the parameters that result in the worst objective magnitude. Then new parameters are selected within the new bounds and replaced by the worst ones: $k_i^{worst} \Leftarrow k_i^{new} \in \left[\tilde{k}_{i\min}, \tilde{k}_{i\max}\right]$ where $\left[\tilde{k}_{i\min}, \tilde{k}_{i\max}\right]$ is new bounds of i^{th} parameter. During the optimization, the initial search spaces given in (35) are updated as:

$$\tilde{X} = \begin{bmatrix} \tilde{k}_{1\min} & \tilde{k}_{1\max} \\ \tilde{k}_{2\min} & \tilde{k}_{2\max} \\ \vdots & \vdots \\ \tilde{k}_{m\min} & \tilde{k}_{m\max} \end{bmatrix} \tag{43}$$

Exchanging the worst parameter of the iteration for the randomly selected new parameter in the corresponding search space increases the probability density of finding optimum parameters as follows:

$$\tilde{f}_{k_i}(\tilde{X}) = \frac{1}{\Delta \tilde{X}} \tag{44}$$

where

$$\Delta \tilde{X} = \begin{bmatrix} \tilde{k}_{1\max} - \tilde{k}_{1\min} \\ \tilde{k}_{2\max} - \tilde{k}_{2\min} \\ \vdots \\ \tilde{k}_{m\max} - \tilde{k}_{m\min} \end{bmatrix} \tag{45}$$

Since $\Delta \tilde{X} < \Delta X$, $\tilde{f}_{k_i}(\tilde{X}) > f_{k_i}(X)$. Therefore, the new parameter selection within the updated bounds of the search space plays an important role on the performance of the PSO.

This article has been accepted for publication in a future issue of this journal, but has not been fully edited. Content may change prior to final publication. Citation information: DOI 10.1109/ACCESS.2022.3177621, IEEE Access

B. IMPLEMENTATION OF THE IMPROVED PSO

Implementations of the traditional and the *improved* PSO algorithms are as follows:

Step 1. Define the bounds of the search spaces for each parameter of the controller and select same number of particles randomly to generate initial positions of particles.

Step 2. Select the initial coefficients of the PSO algorithm:

c_1, c_2 : Acceleration constants,

r_1, r_2 : Random variables between 0-1,

w : Inertia weight,

n : Particle number,

$iter$: Maximum iteration number.

Step 3. Set the particles sequentially to the corresponding parameters of the controller and run the system.

Step 4. *Perform customized objective measurements of the particles of each parameter.*

Step 5. Determine the local best, global best and *local worst* particles of the current iteration.

Step 6. Calculate the velocities of each particle and update the positions of the particles

The velocities of each particle are calculated as follows:

$$v_i(iter+1) = wv_i(iter) + r_1c_1\left(k_i^{lbest} - k_i(iter)\right) + r_2c_2\left(k_i^{gbest} - k_i(iter)\right) \quad (46)$$

where $iter$ is the iteration number of the optimization, v_i is the velocity of the particle $k_i(iter)$. k_i^{lbest} and k_i^{gbest} are local and global best of the particles, respectively.

The particles are updated as follows:

$$k_i(iter+1) = k_i(iter) + v_i(iter+1) \quad (47)$$

Step 7. *Update the bounds of each search space concerning the position of the worst particle of the current iteration.*

Step 8. *Exchange the worst particle of the iteration for the randomly selected new particle in the corresponding search space.*

Step 9. Continue from Step 3 to Step 8 until the iteration number reaches its maximum.

The flowchart of the traditional PSO algorithm shown with solid lines and the improved PSO algorithm shown with the dashed line are depicted in Fig. 4.

C. OBJECTIVE FUNCTION SELECTION

The objective functions for the controller parameters are customized concerning the properties of the controller parameters on the control input and the output of the AVR. Since two parameters are to be optimized, two different objective functions are defined.

In conventional SMC, a large magnitude of switching gain increases the transient response performance of the system while it produces chattering in the control input. Therefore, there is also a dilemma of selecting the appropriate switching gain. For this reason, the following performance rule is proposed to search optimum magnitude of k_{sw}:

$$P_{sw} = \begin{cases} C_d + ISE + t_r & \text{if overshoot exists} \\ ISE + t_r & \text{otherwise} \end{cases} \quad (48)$$

where t_r is the rise time and C_d is the decay coefficient that makes the corresponding particle to be worst and $ISE = \int e^2(t)dt$ which is suitable to suppress large deviation of error.

The equivalent control input plays a vital role in keeping the system at the reference point. For long-period of performance measurement of equivalent control, ITAE is selected for k_0 with the following rule:

$$P_{eq} = \begin{cases} C_d + ITAE & \text{if overshoot exists} \\ ITAE & \text{otherwise} \end{cases} \quad (49)$$

where $ITAE = \int t\left|e(t)\right|dt$ which is helpful to determine the presence of long-term error.

In order to compare the improved PSO with the traditional PSO, the following objective function, including all performance terms of (48) and (49) is constituted for the traditional PSO:

$$P_{traditional} = ITAE + ISE + t_r + OS \quad (50)$$

V. RESULTS AND DISCUSSION

In this section, the optimization results of the proposed sliding mode controllers with both traditional and improved PSO are presented. A second-order approximate model of the AVR can be obtained by using different mathematical methods [76], [77]. Besides, a graphical analysis of the step response of the AVR can be more beneficial for practical applications. First-order and second-order modeling methods based on the step response of a real system were presented in [78]. Since an approximate model of the AVR is adequate for the proposed SMC, the first-order plus dead-time modeling is used to obtain the second-order model of the AVR. In the literature, different orders of AVR models were also studied [31].

The forward path of the AVR is taken into account for the open-loop unit step response, which includes the amplifier, the exciter, and the generator. The sensor is omitted since the gain of the sensor is close to unity [2]. The forward path transfer function is obtained as follows [15]:

$$G_{ForwardPath}(s) = G_a(s)G_e(s)G_g(s)$$

$$G_{ForwardPath}(s) = \left(\frac{10}{0.1s+1}\right)\left(\frac{1}{0.4s+1}\right)\left(\frac{1}{s+1}\right)$$

$$G_{ForwardPath}(s) = \frac{10}{0.04s^3 + 0.54s^2 + 1.5s + 1} \quad (51)$$

This article has been accepted for publication in a future issue of this journal, but has not been fully edited. Content may change prior to final publication. Citation information: DOI 10.1109/ACCESS.2022.3177621, IEEE Access

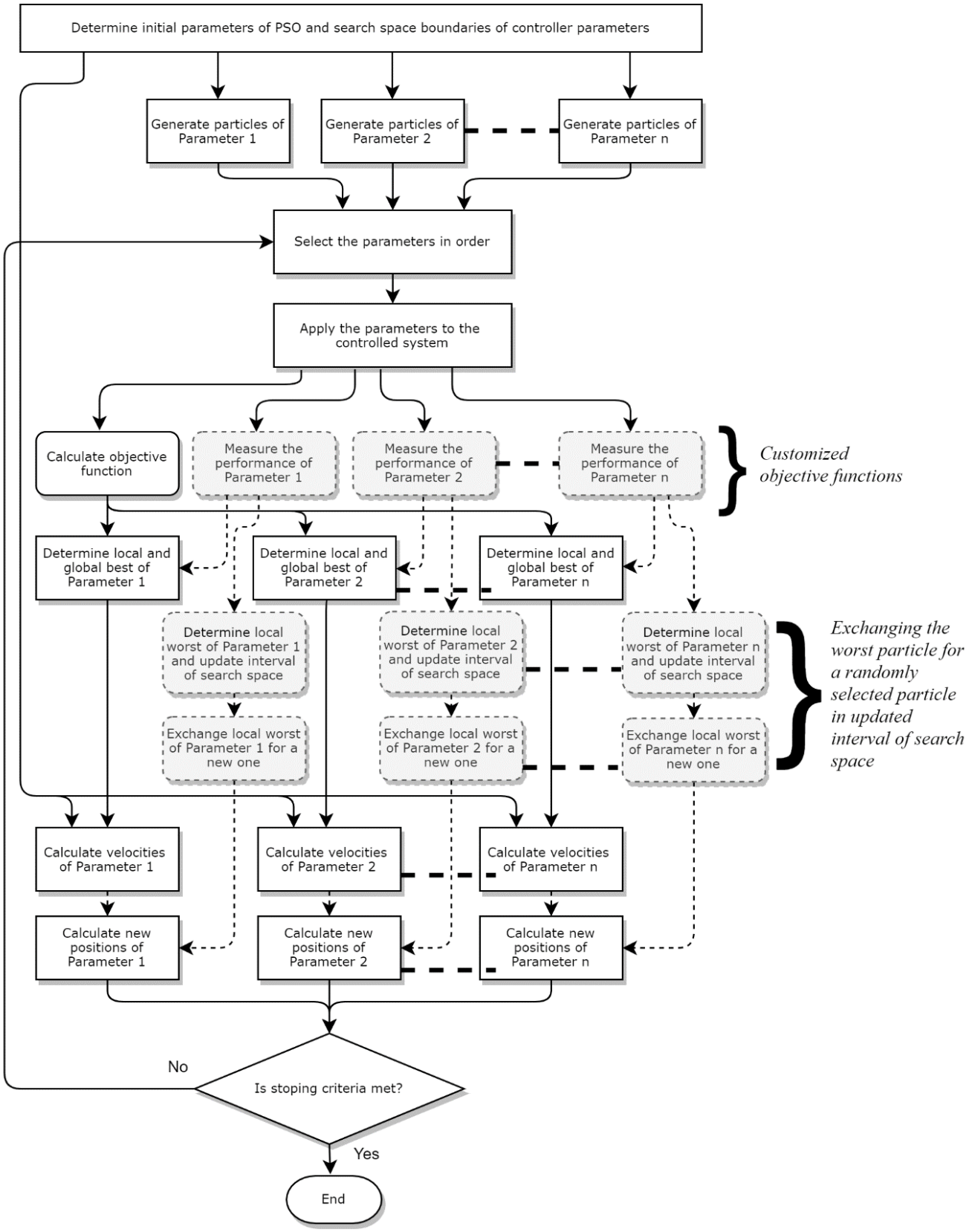

FIGURE 4. **Flowchart of traditional and improved PSO algorithms for n-parameter controller**

This article has been accepted for publication in a future issue of this journal, but has not been fully edited. Content may change prior to final publication. Citation information: DOI 10.1109/ACCESS.2022.3177621, IEEE Access

The second-order approximate transfer function is obtained from the graphical analysis of the unit step response of (51) as follows:

$$G_{AVR}(s) = \frac{19.4567}{s^2 + 3.0295s + 1.9457} \tag{52}$$

The unit step responses of the AVR and the approximate second-order model are depicted in Fig. 5 and the corresponding modeling error is given in Fig. 6. Modeling error according to the transient-state output of the transfer functions is between -2.048% and 2.45%.

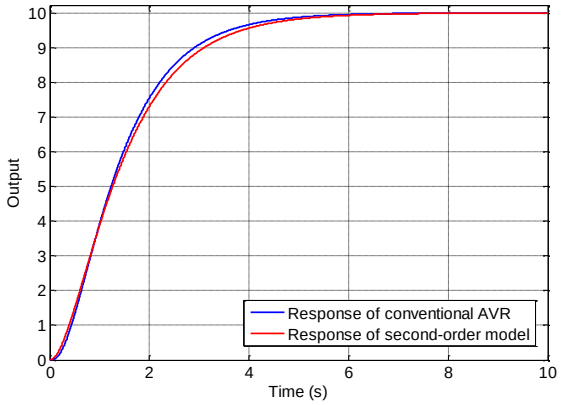

FIGURE 5. Unit step responses of the AVR and its second-order approximate model

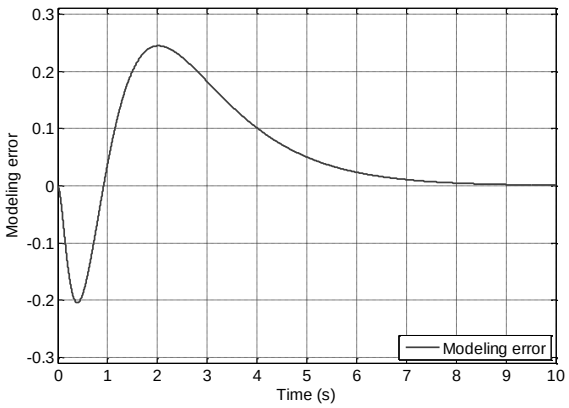

FIGURE 6. Modeling error of the AVR and its second-order approximate model

Remark 5: The number of iteration and population size is directly related to how much an optimization algorithm is realizable. The increase in the number of simulations in the optimization causes it to move away from realization. In other words, it can be recommended to perform optimization that can be done with a small number of simulations. In Table III, simulation numbers are given for comparison.

TABLE III
SIMULATION NUMBERS

Ref. #	Iteration number	Population size	Total number of simulations
[20]	50	300	15000
[46]	100	50	5000
[14]	100	50	5000
[31]	130	25	3250
[16]	100	30	3000
[35]	50	50	2500
[8]	50	50	2500
[28]	50	50	2500
[36]	50	40	2000
[13]	40	40	1600
[11]	50	30	1500
[15]	50	25	1250
[1]	40	30	1200
[4]	20	50	1000
[29]	20	50	1000
[3]	30	30	900
Proposed PSO	***20***	***20***	***400***

According to [73], the exchange of the worst parameter with a new randomly selected parameter increases the probability of finding the global optimum parameters of the controllers by using fewer simulations. Therefore, a small population size with a fewer number of iteration is selected.

A. TRANSIENT RESPONSE ANALYSIS AT NO-LOAD

In the present study, two different structures of controllers are proposed for the AVR by using the second-order approximate model parameters (SMC_2) and third-order open-loop transfer function parameters (SMC_3). In order to present the effect of the limiters, simulations are performed with both conventional AVR (Fig. 1) and the AVR system with limiters (Fig. 3). Furthermore, the effectiveness of improved PSO over traditional PSO is also investigated. All simulations for the transient response analysis are summarized in Fig. 7.

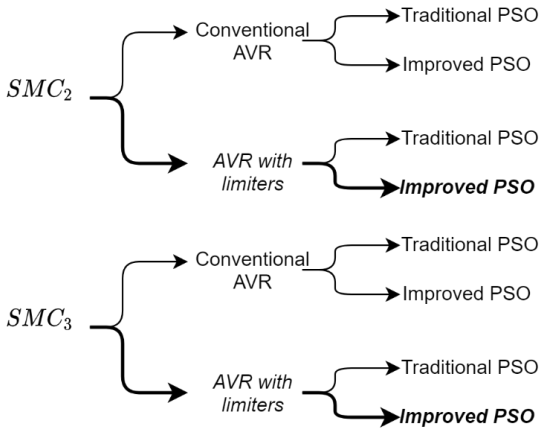

FIGURE 7. All simulations for the proposed controllers and improved PSO

In PSO, there are three parameters that affect the search performance of the algorithm, namely, c_1, c_2, and w. The acceleration constants c_1 and c_2 are used to pull the particles to the local best and the global best positions. In the

literature, different values of the constants have been used. In order to get a balance in the optimization c_1 and c_2 are selected as the same magnitude. The other parameter, w, indicates the inertia weight that enhances the ability of the algorithm. Not only the constant magnitude of w but also linearly changing rules were used in the PSO. Greater magnitude of w may lead to an explosion of the velocity that causes the particles to push out of the search space, while smaller value may cause a slower convergence to the optimal value [79].

In this study, these parameters are chosen so that all particle velocities to local and global positions are balanced. The specifications of the controllers and PSO are listed in Table IV. The optimum controller parameters are shown in Table V. In the optimizations, traditional and improved PSO are run with the same initial positions of the particles.

TABLE IV
INITIAL OPTIMIZATION PARAMETERS

PSO parameters	
Parameter	**Magnitude**
c_1	0.5
c_2	0.5
w	0.5
Search spaces	
k_{sw} for $n=2$	100 – 800
k_0 for $n=2$	0.1 – 0.8
k_{sw} for $n=3$	200 – 2000
k_0 for $n=3$	0.01 – 0.2
Constant parameters	
k_{sf}	0.01
C_d	999
Controller limits	-0.9 – 1.0pu
Exciter saturation factor	3.1pu
Set point	1pu
Simulation duration	3s
Sampling time	1ms

TABLE V
OPTIMUM PARAMETERS OF THE PROPOSED CONTROLLERS

Proposed Controller	AVR System	PSO Type	k_{sw}	k_0
SMC_2	Conventional AVR	Traditional	401.6093	0.6892
		Improved	458.0822	0.6517
	AVR with Limiters	Traditional	594.2612	0.4769
		Improved	431.1797	0.7225
SMC_3	Conventional AVR	Traditional	1889.4	0.1077
		Improved	1528.9	0.1458
	AVR with Limiters	Traditional	1146.5	0.1779
		Improved	1287.5	0.1708

The proposed SMC_2 is used in both AVR systems and optimized with traditional and improved PSO. The corresponding transient responses of the AVR systems are depicted in Fig. 8. Similarly, the response of the SMC3 for each AVR system and optimization algorithms are shown in Fig. 9.

It is noteworthy that the AVR outputs in the transient-state are disturbed by the limiters introduced for the controller and the exciter as seen in Fig. 8 and Fig. 9. This is because the evaluated control input is cropped at the controller and the exciter outputs.

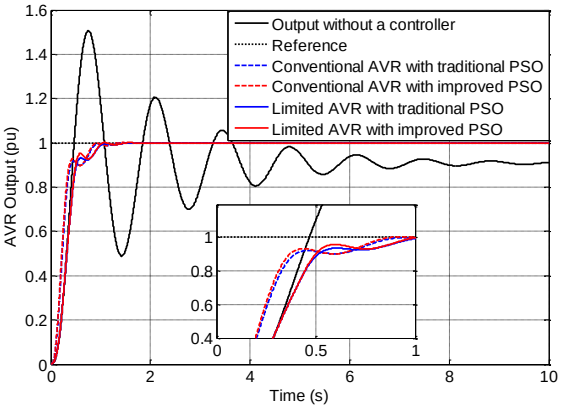

FIGURE 8. Transient responses of the AVR systems with SMC_2

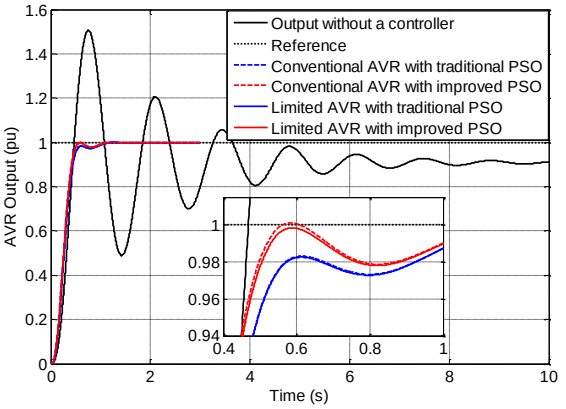

FIGURE 9. Transient responses of the AVR systems with SMC_3

Although the proposed controllers generate the necessary control input, the limiters became barriers to the desired fast response. Despite these obstacles, a good controller performance has been achieved. The corresponding control inputs generated by the proposed controllers are shown in Fig. 10 and Fig. 11. The calculated control inputs of the proposed controllers cropped at 1pu because of the controller limiters.

This article has been accepted for publication in a future issue of this journal, but has not been fully edited. Content may change prior to final publication. Citation information: DOI 10.1109/ACCESS.2022.3177621, IEEE Access

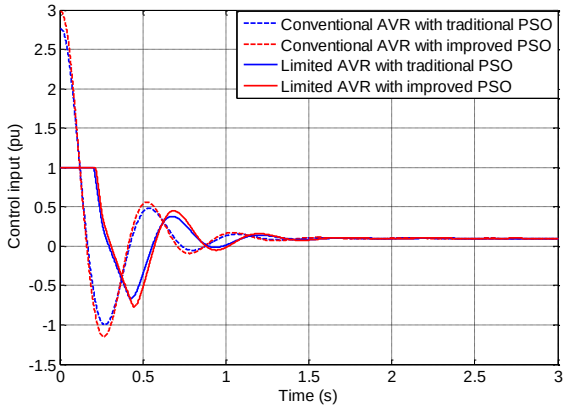

FIGURE 10. Control inputs of SMC_2

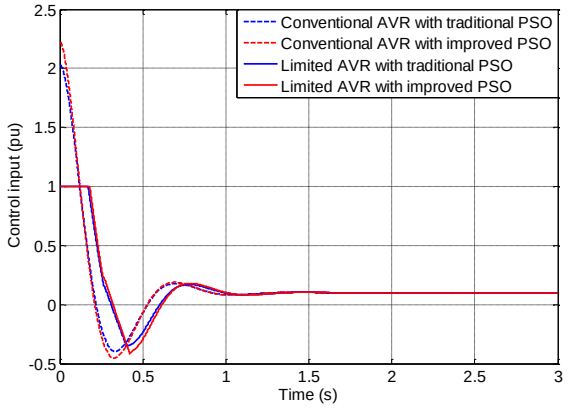

FIGURE 11. Control inputs of SMC_3

It is clearly seen that the calculated control inputs are cropped by the limiter at 1pu. Another limiter, introduced at the output of the exciter, is also affected the excitation of the generator. In Fig. 12 and Fig. 13, the excitation signals of the generator in the transient-state are depicted for SMC_2 and SMC_3, respectively.

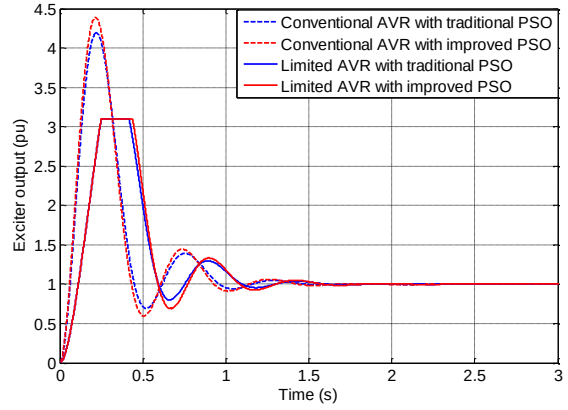

FIGURE 12. Exciter outputs when using SMC_2

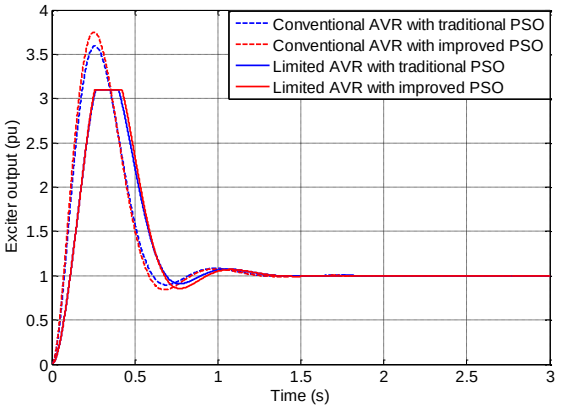

FIGURE 13. Exciter outputs when using SMC_3

A slight delay can be seen at the exciter outputs since the control input is cropped at 1pu. In addition, the exciter limiter at 3.1pu also reduces the excitation. Therefore, as seen in Fig. 8 and Fig. 9, the step response of the AVR with limiters is slower as compared with the response of the conventional AVR. In Table VI, time domain specifications are given. In general, better results were obtained when using the improved PSO for each controller and the AVR system.

TABLE VI
TIME DOMAIN SPECIFICATIONS OF TRANSIENT-STATES OF AVR OUTPUTS

Proposed Controller	AVR System	PSO Type	Rise Time	Settling Time (±2%)	OS %
SMC_2	Conventional AVR	Traditional	0.3705	0.9701	0
		Improved	0.3552	0.9537	0
	AVR with Limiters	Traditional	0.3610	0.9643	0
		Improved	0.3441	0.9479	0.09
SMC_3	Conventional AVR	Traditional	0.3181	0.9252	0
		Improved	0.2969	0.8726	0.1
	AVR with Limiters	Traditional	0.3179	0.9259	0
		Improved	0.2998	0.8819	0.08

In the optimization of the traditional PSO, a single objective function is defined, $P_{traditional}$, in (50). However, individual objective functions are defined for each parameter of the proposed controller in the improved PSO, P_{sw} in (48) and P_{eq} in (49). The tracking performance of $P_{traditional}$, P_{sw}, and P_{eq} are given in Fig. 14, Fig. 15, and Fig. 16, respectively. As seen in Fig. 15 and Fig. 16, the magnitude of objective functions decreases rapidly in the first quarter of the total iteration, and fine-tuning is observed in the remaining iterations.

This article has been accepted for publication in a future issue of this journal, but has not been fully edited. Content may change prior to final publication. Citation information: DOI 10.1109/ACCESS.2022.3177621, IEEE Access

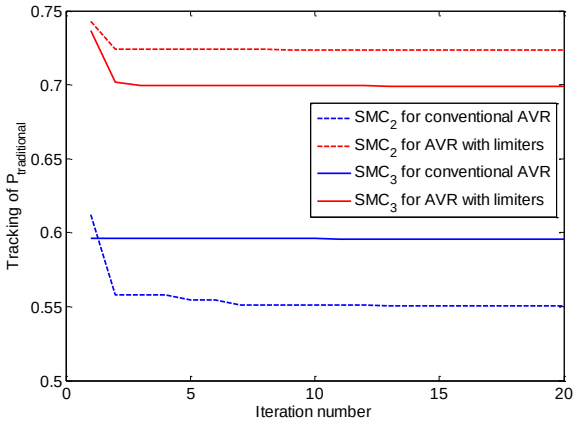

FIGURE 14. **Objective function tracking performance of the traditional PSO, $P_{traditional}$**

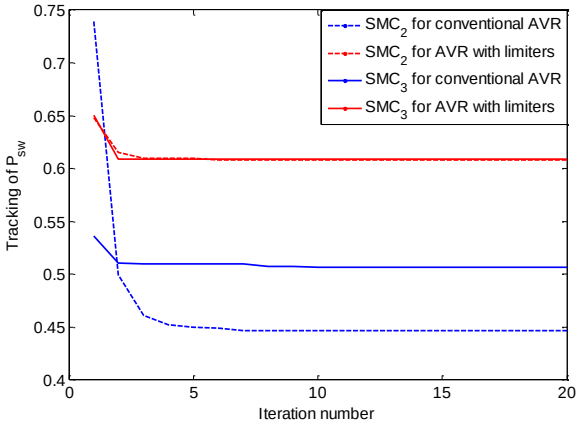

FIGURE 15. **Objective function tracking performance of the improved PSO for k_{sw}, P_{sw}**

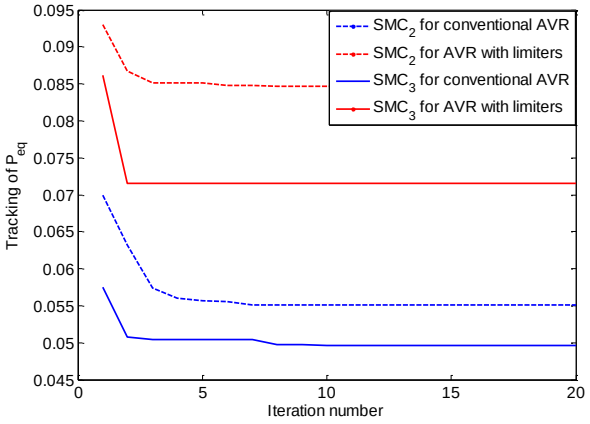

FIGURE 16. **Objective function tracking performance of the improved PSO for k_0, P_{eq}**

The initial control input to the amplifier is at maximum allowable magnitude. Therefore, the exciter runs at the maximum. The sum of switching and equivalent control laws exceeds the upper bound of the limiters. Both control laws produced by SMC_2 and SMC_3 are shown in Fig. 17 and Fig. 18, respectively. As seen in the following figures, the chattering phenomenon of SMC is eliminated in the proposed controller schemes.

It is clearly seen that the controller is activated by the switching control laws in the transient-state by the nature of SMC theory. As the system states converge to the desired values, the magnitudes of switching controls converge to zero until the system is affected by any disturbance or uncertainties.

The proposed controllers generated the switching controls without chattering, as seen in Fig. 17 and Fig. 18. Besides, larger control inputs are generated using the controller parameters obtained from the improved PSO compared with the result of traditional PSO. At the end of the transient-state, all the switching controls converged to zero as expected.

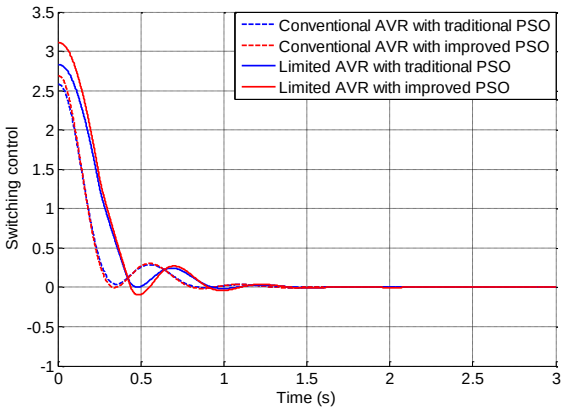

FIGURE 17. **The switching control of SMC_2**

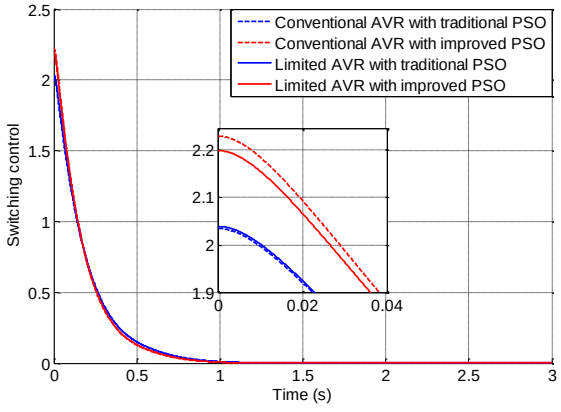

FIGURE 18. **The switching control of SMC_3**

In the steady-state, the equivalent controls drove the system as seen in Fig. 19 and Fig. 20. In the steady-state, the system was driven by the equivalent control laws, while the switching control was dominant in the transient-state.

This article has been accepted for publication in a future issue of this journal, but has not been fully edited. Content may change prior to final publication. Citation information: DOI 10.1109/ACCESS.2022.3177621, IEEE Access

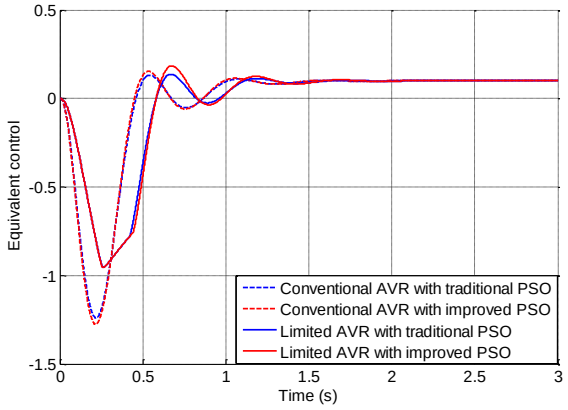

FIGURE 19. The equivalent control of SMC_2

The relative degree of the proposed controllers is 1, and the stability of the controllers is guaranteed in the sense of the Lyapunov stability theorem. Fig. 21 and Fig. 22 clearly show that the sliding surface functions converge to zero in a finite time.

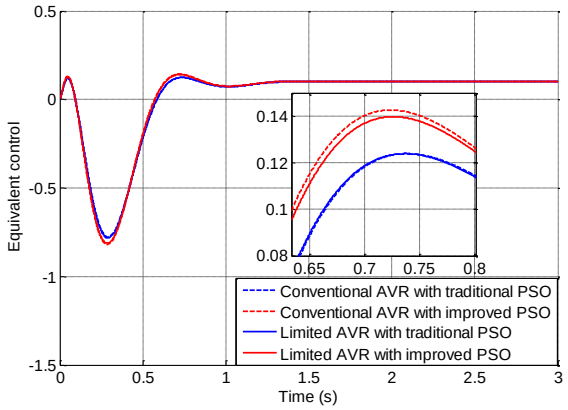

FIGURE 20. The equivalent control of SMC_3

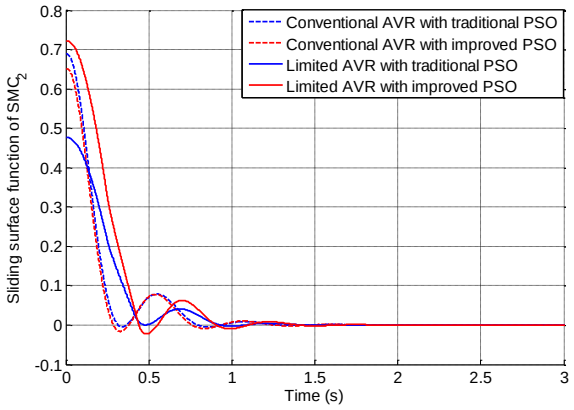

FIGURE 21. Tracking of sliding surface function of SMC_2

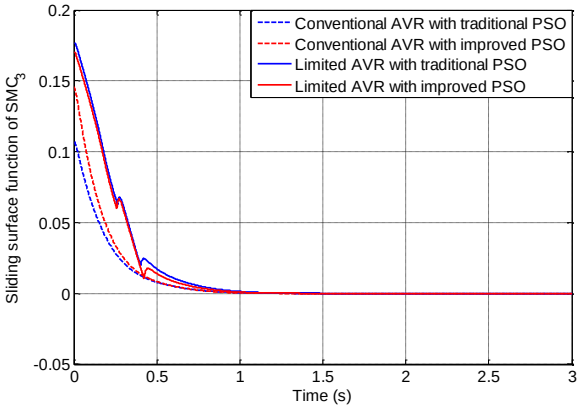

FIGURE 22. Tracking of sliding surface function of SMC_3

In this section, a comprehensive analysis of the proposed SMC_2 and SMC_3 controllers was evaluated on the conventional AVR and the AVR with limiters. The negative effect of the limiters is seen in the figures reflected in the outputs of the system, the control inputs, and the tracking performance of the sliding surface functions. Despite the obstacle of the limiters, both the proposed controllers and the improved PSO have successfully brought the output of the system to the desired value.

In the remaining sections, the results of SMC_2 and SMC_3 optimized with the improved PSO for the AVR system with limiters are used.

B. PERFORMANCE COMPARISON AT NO-LOAD

In the literature, the performance of the proposed controllers is commonly compared with the time-domain specifications as maximum peak value (M_p), overshoot ($OS\%$), rise time (t_r, from 10% to 90%), settling time (±2% or ±5% band). Besides, the error-based performance indices (ISE, ITSE, IAE, ITAE) were also evaluated to indicate the superiority of the proposed controllers and corresponding optimization algorithms [16].

It is clear that the performance of the controllers with limiters is different than the proposed controllers without having any limiters. The biggest challenge in claiming a good performance is to provide all the performance indices in balance. As stated in [16], minimum rise time results in a larger overshoot. However, when there is no overshoot at the output, a long rise time is observed. It is noteworthy that the overshoot at the output is not desired feed-back control systems but may be acceptable if it is less than 5% of the desired terminal voltage [35].

In the present study, the overshoot is limited at 0.1% of the desired terminal voltage in the definitions of objective functions since a larger overshoot deviates the terminal voltage causing a large variation in reactive power flow. In order to figure out the whole performance of the proposed controllers in a fair manner, not only the effect of limiters must be included in the evaluation, but also the performance

This article has been accepted for publication in a future issue of this journal, but has not been fully edited. Content may change prior to final publication. Citation information: DOI 10.1109/ACCESS.2022.3177621, IEEE Access

of the optimization must be considered. In Table VII, the reported time-domain specifications from cited studies are given to compare with the proposed SMC performance.

TABLE VII
PERFORMANCE COMPARISON WITH TIME-DOMAIN SPECIFICATIONS

Ref #	*OS%*	Rise time (s)	Settling time (s) (±2% band)	Settling time (s) (±5% band)
SMC_2	0.09	0.3441	0.9479	0.8635
SMC_3	0.08	0.2998	0.8812	0.4632
The reported time-domain specifications from the cited studies				
[46]	1.00	0.3537	0.5603	--
[14]	15.57	0.1310	--	0.7580
[31]*	0	4.7400	--	22.310
[16]	1.98	0.2502	--	0.3733
[35]	13.20	0.0827	0.4530	--
[8]*	1.17	0.2768	--	0.4027
[28]*	2.22	0.6900	3.4420	--
[36]	0.61	0.3149	0.4817	--
[13]	22.80	0.1030	--	0.5840
[11]	2.60	0.2400	--	0.5200
[15]	0	0.3234	--	0.5028
[1]	15.00	0.1280	0.7530	--
[4]	12.80	0.1900	--	0.9000
[29]*	2.02	--	3.3123	--
[3]	1.30	0.3530	--	0.4850
[20]	25.00	0.1560	--	0.9200

* One of the proposed controller responses was included.

It can be concluded from Table VII that the proposed controller having two parameters exhibits good performance at the no-load condition. Another remark to note is that the overshoot is under 0.1% without sacrificing the rise time and settling time.

C. ROBUSTNESS EVALUATION AGAINST UNCERTAIN PARAMETERS

The properties of AVR constituents vary due to the load variations and aging in their lifetime [2]. Therefore, robustness against parameter uncertainties and load at the generator terminal was evaluated in the literature. The time constants of the AVR constituents were changed and the corresponding step responses were reported as either graphically or giving time-domain specifications [1], [3], [10], [11], [13], [14], [17], [19], [35], [46]. Generally, the time constants were changed with 25% steps from -50% to 50%.

Similar to the literature, the performance of the proposed controllers is evaluated. In Table VIII, the robustness analysis of SMC_2 against parameters uncertainties is given and corresponding outputs are depicted in Figs. 23-26.

TABLE VIII.
PARAMETER UNCERTAINTY ROBUSTNESS MEASUREMENTS OF SMC_2

AVR constituent	Time constant change	*OS%*	Rise time (s)	Settling time (s) (±2% band)	Settling time (s) (±5% band)
Amplifier, τ_a	-50%	0	0.4536	0.9056	0.7363
	-25%	0	0.3690	0.9004	0.7907
	+25%	0	0.4657	0.8908	0.7093
	+50%	2.3824	0.3409	1.2781	1.0107
Exciter, τ_e	-50%	0	0.5285	1.0140	0.7279
	-25%	0.0153	0.3478	0.8732	0.8021
	+25%	0.4693	0.3504	1.0217	0.9014
	+50%	0.6291	0.3596	1.0939	0.5810
Generator, τ_g	-50%	0.0243	0.4752	0.9534	0.6627
	-25%	0.0261	0.5245	0.8314	0.7567
	+25%	2.2034	0.4026	1.0993	0.6052
	+50%	6.5389	0.4755	1.2571	0.9041
Sensor, τ_s	-50%	0.0122	0.3512	0.9483	0.8470
	-25%	0.0488	0.3474	0.9478	0.8552
	+25%	0.3335	0.3413	0.9487	0.8718
	+50%	0.6120	0.3390	0.9503	0.8802

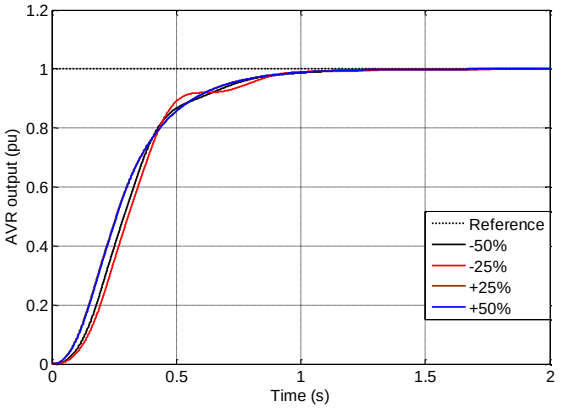

FIGURE 23. Effect of amplifier time-constant uncertainties on the AVR output with SMC_2

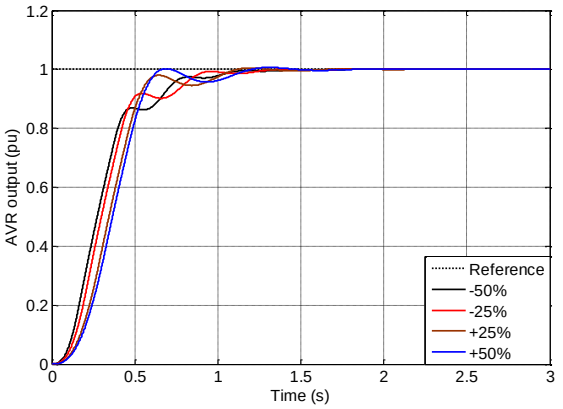

FIGURE 24. Effect of exciter time-constant uncertainties on the AVR output with SMC_2

This article has been accepted for publication in a future issue of this journal, but has not been fully edited. Content may change prior to final publication. Citation information: DOI 10.1109/ACCESS.2022.3177621, IEEE Access

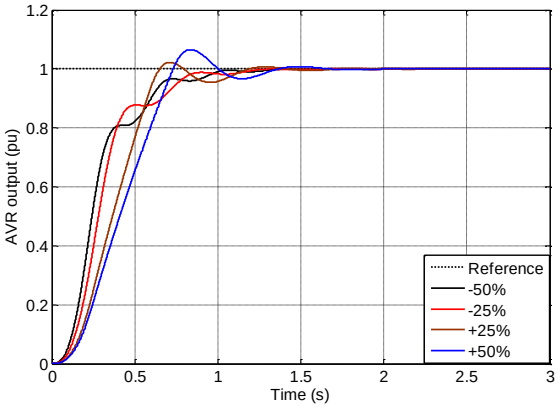

FIGURE 25. Effect of generator time-constant uncertainties on the AVR output with SMC$_2$

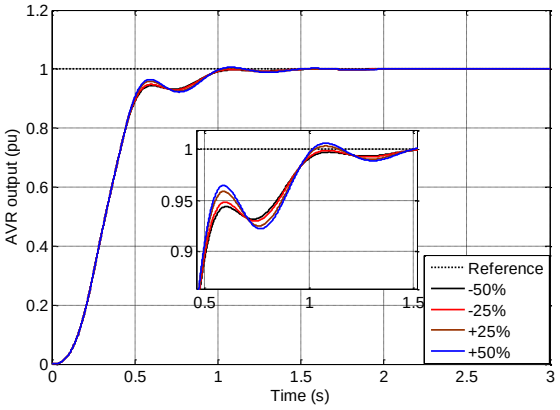

FIGURE 26. Effect of sensor time-constant uncertainties on the AVR output with SMC$_2$

Similarly, the robustness analysis of SMC$_3$ against parameter uncertainties are given in Table IX, and corresponding outputs are depicted in Figs. 27-30. All the measurements are performed with the optimized parameters of the proposed controllers given in Table IV.

TABLE IX
PARAMETER UNCERTAINTY ROBUSTNESS MEASUREMENTS OF SMC$_3$

AVR constituent	Time constant change	*OS%*	Rise time (s)	Settling time (s) (±2% band)	Settling time (s) (±5% band)
Amplifier, τ_a	-50%	0	0.3901	0.7593	0.6191
	-25%	0	0.3595	0.7065	0.5726
	+25%	3.0879	0.3417	1.1045	0.5427
	+50%	6.0100	0.3425	1.2063	0.7571
Exciter, τ_e	-50%	0	0.3755	0.8733	0.7237
	-25%	0	0.3434	0.9161	0.5518
	+25%	2.9846	0.3537	0.8080	0.5621
	+50%	5.3886	0.3651	0.9453	0.8171
Generator, τ_g	-50%	0	0.3782	0.8234	0.6887
	-25%	0	0.3274	0.8908	0.5574
	+25%	5.0661	0.4027	0.9190	0.7876
	+50%	8.3750	0.4756	1.1195	1.0302
Sensor, τ_s	-50%	0.0378	0.3509	0.6055	0.5562
	-25%	0.0589	0.3481	0.5960	0.5511
	+25%	0.4586	0.3431	0.9603	0.5415
	+50%	0.8451	0.3409	0.9872	0.5371

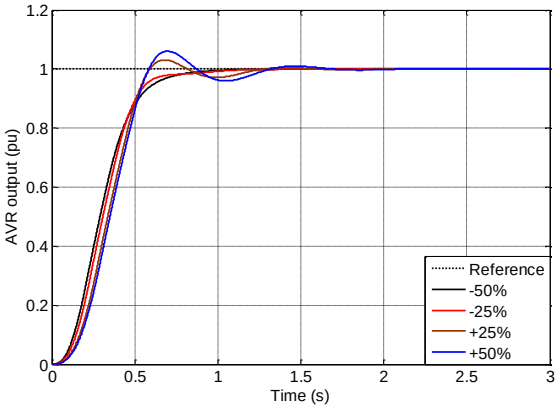

FIGURE 27. Effect of amplifier time-constant uncertainties on the AVR output with SMC$_3$

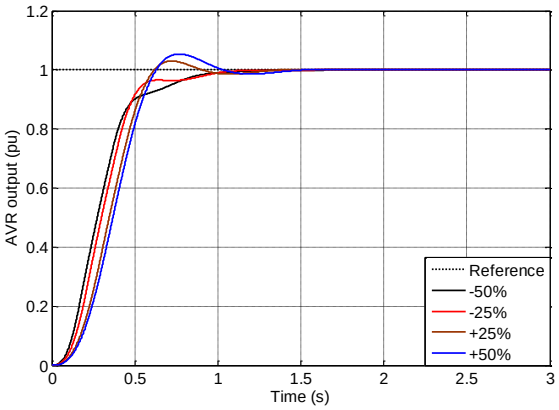

FIGURE 28. Effect of exciter time-constant uncertainties on the AVR output with SMC$_3$

As seen in the figures related to the robustness of the proposed controllers, the stability is kept in the event of uncertain parameters. The output of the AVR changes slightly. At the end of transient-state, no steady-state error was observed.

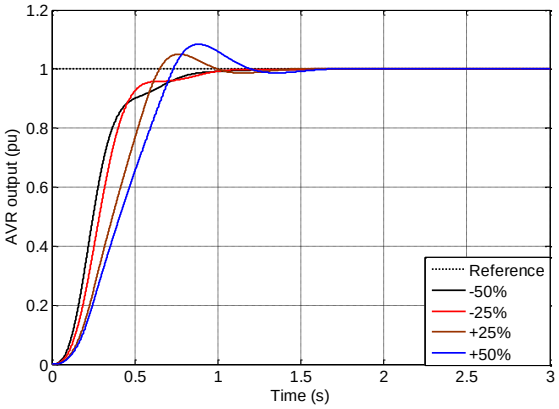

FIGURE 29. Effect of generator time-constant uncertainties on the AVR output with SMC$_3$

This article has been accepted for publication in a future issue of this journal, but has not been fully edited. Content may change prior to final publication. Citation information: DOI 10.1109/ACCESS.2022.3177621, IEEE Access

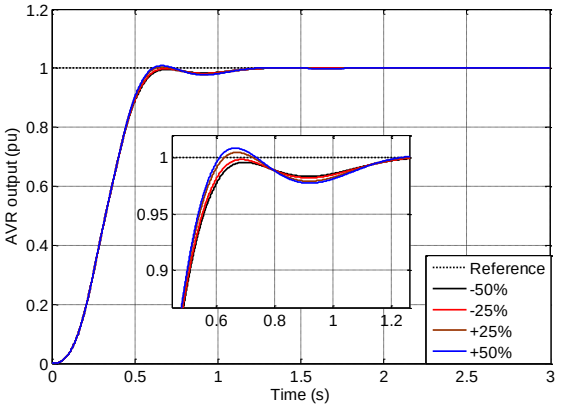

FIGURE 30. Effect of sensor time-constant uncertainties on the AVR output with SMC_3

A comprehensive comparison can present how the proposed controllers recover the output subjected to parameter uncertainties. Since the overshoot changes the direction of power flow, a new comparison criterion is considered. Concerning the uncertainty interval of the AVR constituents from -50% to +50% changes in the time constants, the average overshoot rate shows how much the controllers generate an accurate control input in that interval.

In the present study, the average overshoot rates of the controllers in Table X are also calculated. It is clearly seen from the results that the proposed SMC schemes are most robust to parametric uncertainties. The proposed controllers generate the most negligible overshoot at the generator terminal. The results proved the superiority of SMC_2 and SMC_3 over the compared controllers in the sense of robustness against the parameter uncertainties.

D. ROBUSTNESS EVALUATION AGAINST LOAD DISTURBANCE

Another robustness criterion for the AVR control is the load disturbance rejection capability of the controllers. Less than 5% of rated terminal voltage deviation may be allowable [35] but the controller should suppress the disturbance even if more than 5%. In the literature, the disturbance rate is generally selected as ±10% of rated terminal voltage [14], [16], [24]. In Fig. 31, the injected disturbance and the corresponding the AVR outputs are depicted for SMC_2 and SMC_3. +0.1pu disturbance is applied at 2s and removed at 4s, then -0.1pu disturbance is applied at 6s and removed at 8s. Since 0.1pu step disturbance is injected, the initial measurement starts with the magnitude of the step, and then the output enters and remains in the ±5% error band in less than 0.4s.

TABLE X
COMPARISON OF OVERSHOOT RATES OF THE CONTROLLERS SUBJECTED TO PARAMETER UNCERTAINTIES

AVR constituent	Time constant change	*OS%* of SMC_2	*OS%* of SMC_3	*OS%* in [1]	*OS%* in [35]	*OS%* in [10]	*OS%* in [11]	*OS%* in [14]	*OS%* in [19]	*OS%* in [20]	*OS%* in [29]*
Amplifier τ_a	-50%	0	0	4.90	16.90	0	1.83	4.68	6.781	11	5.8606
	-25%	0	0	10.90	15.20	0	1.88	11.12	10.685	19	3.6030
	+25%	0	3.0879	18.00	10.60	3.84	6.40	18.83	0.458	28	0.4888
	+50%	2.3824	6.0100	20.30	6.85	6.80	9.50	21.35	0.440	33	0.2812
Exciter τ_e	-50%	0	0	21.80	8.18	0	1.45	21.27	5.625	24	0
	-25%	0.0153	0	17.90	10.20	0	1.87	18.09	3.006	22	1.5430
	+25%	0.4693	2.9846	12.80	17.50	3.28	4.28	13.57	0.030	25	1.5029
	+50%	0.6291	5.3886	11.10	24.20	5.88	6.25	12.28	0.232	26	5.5729
Generator τ_g	-50%	0.0243	0	30.60	4.82	5.16	10.92	30.08	3.770	34	3.1916
	-25%	0.0261	0	21.40	8.34	1.79	5.69	21.56	1.890	27	4.6066
	+25%	2.2034	5.0661	10.20	20.10	1.11	3.61	10.93	2.118	22	1.3990
	+50%	6.5389	8.3750	6.50	30.70	3.11	5.44	7.63	6.147	20	1.1751
Sensor τ_s	-50%	0.0122	0.0378	12.10	17.70	0	1.93	12.78	1.308	21	0.1970
	-25%	0.0488	0.0589	13.60	15.40	0	2.24	14.15	0.875	23	1.7421
	+25%	0.3335	0.4586	16.40	11.10	1.00	3.38	17.03	0.475	26	3.0307
	+50%	0.6120	0.8451	18.00	9.12	1.36	4.01	18.52	0.473	27	2.0857
Average OS% Comparison		*OS%* of SMC_2	*OS%* of SMC_3	*OS%* in [1]	*OS%* in [35]	*OS%* in [10]	*OS%* in [11]	*OS%* in [14]	*OS%* in [19]	*OS%* in [20]	*OS%* in [29]*
		0.8309	*2.0195*	*15.4063*	*14.1819*	*2.0831*	*4.4175*	*15.8669*	*2.7696*	*24.250*	*2.2675*

*In [29], the controller was re-optimized for each time constant change in AVR constituent.

This article has been accepted for publication in a future issue of this journal, but has not been fully edited. Content may change prior to final publication. Citation information: DOI 10.1109/ACCESS.2022.3177621, IEEE Access

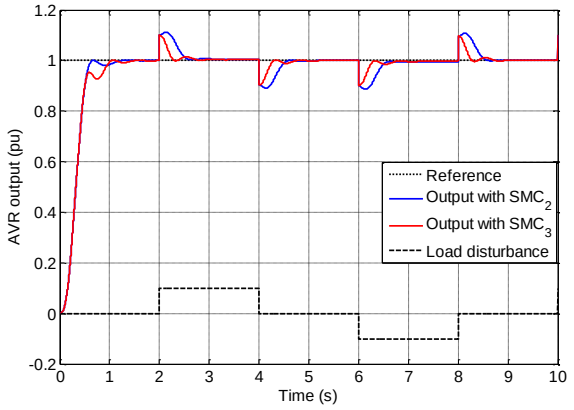

FIGURE 31. Load disturbance rejection of SMC_2 and SMC_3

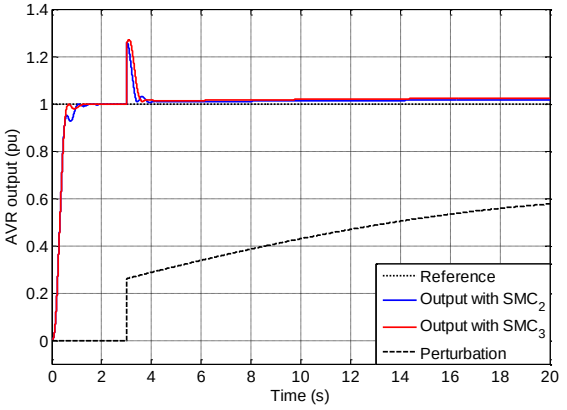

FIGURE 32. Recovery of AVR output for an abrupt incremented fault (Scenario 1)

E. ROBUSTNESS EVALUATION AGAINST ABRUPT AND FOLLOWED BY MONOTONICALLY CHANGING DISTURBANCE

In the event of a sudden failure, a large increase or decrease in the magnitude of the voltage may occur. Furthermore, this failure may continue monotonously. In such fault situations, the accurate control input is particularly critical to keep the output voltage at the reference value. In order to evaluate the robustness of the proposed controllers, the following scenarios are applied to the AVR system.

Scenario 1: An abrupt change then monotonically increasing output

Assume that there is a fault that increases the voltage of the distribution network abruptly and then it increases continuously. In this case, the AVR system should be able to stabilize the output at the reference value. For this scenario, the output of the AVR is increased more than 25% of the reference at 3rd second and then monotonically increased up the 60% during the remaining 17s. The response of the AVR system with both controllers is depicted in Fig. 32. It is clearly seen from the figure that the controller recovers the abrupt change in 1s. In addition, the maximum errors measured at 20th second are 0.019pu for SMC_2 and 0.027pu for SMC_3.

There are two obstacles to recovering the output voltage in the present study, namely, the limiters. The outputs of SMC_2 and SMC_3 controllers and exciter outputs corresponding to the fault in this scenario are depicted in Fig. 33 and Fig. 34, respectively. The monotonic increase is well covered by the controllers.

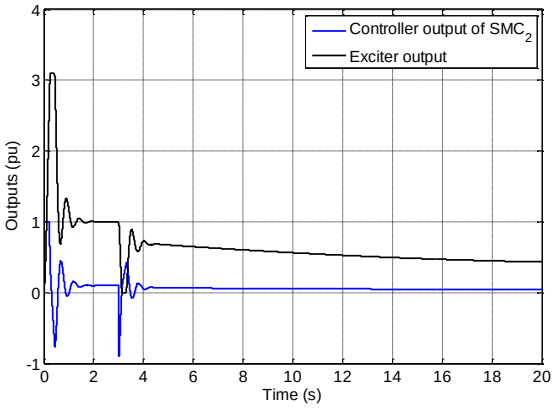

FIGURE 33. Outputs of SMC_2 and exciter for Scenario 1

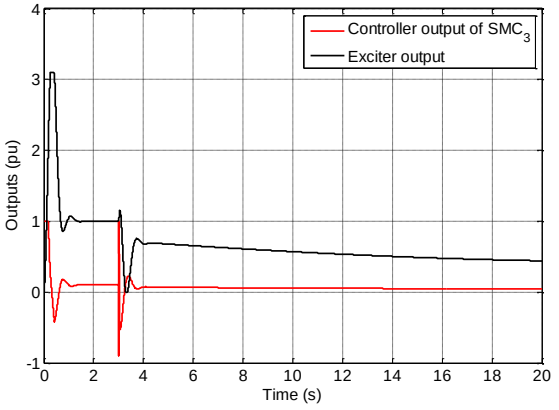

FIGURE 34. Outputs of SMC_3 and exciter for Scenario 1

Scenario 2: An abrupt change then monotonically decreasing output

This scenario is the reverse of the first one. In this scenario, a decrement at 3rd second is seen, and the voltage is reduced monotonically to down to 60% of the reference. The proposed controllers generate the accurate control inputs to recover the abrupt change in 1s as in the previous fault.

Although the fault is continuous, the proposed controllers generate the accurate control inputs so that the maximum errors at 20th second are 0.019pu for SMC_2 and 0.027pu for SMC_3. The corresponding output of the AVR system with both controllers is depicted in Fig. 35.

This article has been accepted for publication in a future issue of this journal, but has not been fully edited. Content may change prior to final publication. Citation information: DOI 10.1109/ACCESS.2022.3177621, IEEE Access

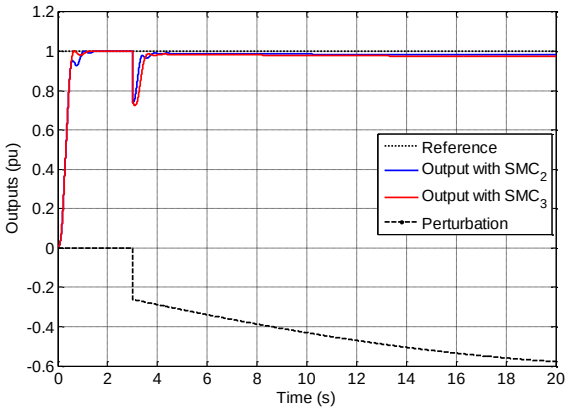

FIGURE 35. Recovery of AVR output for an abrupt decremented fault (Scenario 2)

In this fault scenario, only the outputs of the controllers are affected by the limiters. The necessary excitation outputs are within limits. The generated outputs by SMC_2 and SMC_3 are shown in Fig. 36 and Fig. 37, respectively.

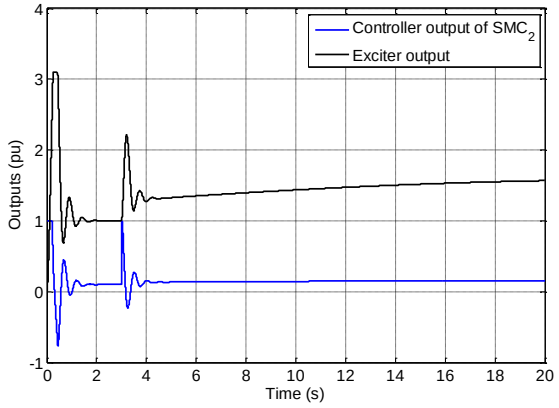

FIGURE 36. Outputs of SMC_2 and exciter for Scenario 2

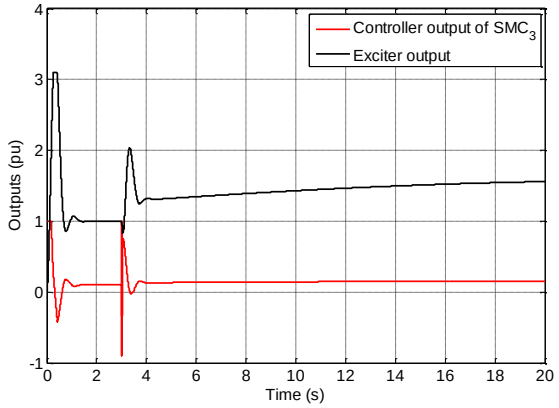

FIGURE 37. Outputs of SMC_3 and exciter for Scenario 2

These two scenarios show that the proposed controllers subject to the limiters are robust against whether the sharp change or monotonic change occurs is seen at the distribution line. The absolute error measured at the end of the two scenarios is less than 5% even if the perturbation at the output reaches nearly ±60% of its nominal value.

Obviously, the performance of a controller optimized for a nominal operating point does not guarantee robustness during its lifetime [2]. Therefore, designed SMC_2 and SMC_3 optimized for a nominal operating point are evaluated without changing controller parameters. From the results above, the proposed controllers exhibit reliable performance against parameter uncertainties and load disturbances. The controllers generate fast and accurate control inputs to maintain the output at the rated value.

The AVR efficiency, which decreases with the effect of aging, is also investigated in this study. The forward-path gain of the AVR is reduced by 10%, 20%, and 30% of its nominal value. Then, the proposed controllers optimized for the nominal operating point are still able to generate accurate control inputs that result in no steady-state error at the generator terminal.

VI. CONCLUSIONS

In the present study, two sliding mode controllers were designed and implemented to control AVR in the presence of parametric uncertainties and load disturbances. Unlike the studies in the literature, limiters were used to limit the control input. A saturation factor was introduced at the output of the controller and the exciter in accordance with the direction of IEEE standards.

A systematic design procedure of control inputs was described in detail. A novel rule for sliding surfaces was proposed that varied with respect to the degree of the controlled system. The stability of the proposed controllers was guaranteed by Lyapunov stability theorem concerning the lumped uncertainties. Only two controller parameters were optimized with the improved PSO. Due to its simplicity, minimum population size and iteration were used in the optimization. Therefore, the computational cost was also minimized.

Although the limiters caused a delay in the output of the controllers and exciters, the performance of AVR was considerably kept well as compared to the conventional AVR. Besides, the new features of the improved PSO enhanced the optimization of controllers.

The well-known drawback of the SMC schemes, chattering, was reduced by using a frequently preferred smooth function, hyperbolic tangent, in the switching control law.

The performance of the proposed controllers was also compared with the recently published studies. The results of the identical operating conditions showed that the proposed controllers generated more accurate control input. The overshoot at the output was minimized without sacrificing

the transient performance. Although the forward gain of the AVR was reduced concerning the effect of the aging factor, there was no steady-state error observed at the output. Further analysis on the robustness was performed for the abrupt and monotonic changes at the output of the AVR. The proposed controllers generated accurate control inputs so that the error at the output is less than 5% of its nominal value.

Finally, two new sliding mode controllers were designed for the AVR in agreement with IEEE excitation limiters. Owing to the excellent outcomes given in graphically and statistically verified that the proposed controllers are stable and robust against parametric uncertainties, load disturbances and decreasing efficiency. Since most AVR studies focused on the PID controller, SMC can be a good alternative to PID as a new controller.

The systematic design procedure and the results of the proposed SMC schemes provide a good starting point for the application of SMC schemes on the AVR system and encourage us to investigate the performance of other SMC schemes in the future. Since the switching control law is dominant in the transient-state, evaluation of the performance of other smooth control laws is another aim of our future studies.

REFERENCES

[1] S. Ekinci and B. Hekimoglu, "Improved Kidney-Inspired Algorithm Approach for Tuning of PID Controller in AVR System," *IEEE Access*, vol. 7, pp. 39935–39947, 2019, doi: 10.1109/ACCESS.2019.2906980.

[2] M. Modabbernia, B. Alizadeh, A. Sahab, and M. M. Moghaddam, "Robust control of automatic voltage regulator (AVR) with real structured parametric uncertainties based on H∞ and μ-analysis," *ISA Trans.*, vol. 100, pp. 46–62, 2020, doi: 10.1016/j.isatra.2020.01.010.

[3] E. Çelik and R. Durgut, "Performance enhancement of automatic voltage regulator by modified cost function and symbiotic organisms search algorithm," *Eng. Sci. Technol. an Int. J.*, vol. 21, no. 5, pp. 1104–1111, 2018, doi: 10.1016/j.jestch.2018.08.006.

[4] Y. Zhou, J. Zhang, X. Yang, and Y. Ling, "Optimization of PID controller based on water wave optimization for an automatic voltage regulator system," *Inf. Technol. Control*, vol. 48, no. 1, pp. 160–171, 2019, doi: 10.5755/j01.itc.48.1.20296.

[5] M. Elsisi, "New design of robust PID controller based on meta-heuristic algorithms for wind energy conversion system," *Wind Energy*, vol. 23, no. 2, pp. 391–403, 2020, doi: 10.1002/we.2439.

[6] M. Elsisi, "Optimal design of nonlinear model predictive controller based on new modified multitracker optimization algorithm," *Int. J. Intell. Syst.*, vol. 35, no. 11, pp. 1857–1878, 2020, doi: 10.1002/int.22275.

[7] M. Elsisi, M. Q. Tran, H. M. Hasanien, R. A. Turky, F. Albalawi, and S. S. M. Ghoneim, "Robust model predictive control paradigm for automatic voltage regulators against uncertainty based on optimization algorithms," *Mathematics*, vol. 9, no. 22, 2021, doi: 10.3390/math9222885.

[8] Z. L. Gaing, "A particle swarm optimization approach for optimum design of PID controller in AVR system," *IEEE Trans. Energy Convers.*, vol. 19, no. 2, pp. 384–391, 2004, doi: 10.1109/TEC.2003.821821.

[9] H. M. Hasanien, "Design optimization of PID controller in automatic voltage regulator system using taguchi combined genetic algorithm method," *IEEE Syst. J.*, vol. 7, no. 4, pp. 825–831, 2013, doi: 10.1109/JSYST.2012.2219912.

[10] P. K. Mohanty, B. K. Sahu, and S. Panda, "Tuning and assessment of proportional-integral-derivative controller for an automatic voltage regulator system employing local unimodal sampling algorithm," *Electr. Power Components Syst.*, vol. 42, no. 9, pp. 959–969, 2014, doi: 10.1080/15325008.2014.903546.

[11] M. A. Sahib and B. S. Ahmed, "A new multiobjective performance criterion used in PID tuning optimization algorithms," *J. Adv. Res.*, vol. 7, no. 1, pp. 125–134, 2016, doi: 10.1016/j.jare.2015.03.004.

[12] S. Kansit and W. Assawinchaichote, "Optimization of PID Controller Based on PSOGSA for an Automatic Voltage Regulator System," *Procedia Comput. Sci.*, vol. 86, no. March, pp. 87–90, 2016, doi: 10.1016/j.procs.2016.05.022.

[13] E. Çelik, "Incorporation of stochastic fractal search algorithm into efficient design of PID controller for an automatic voltage regulator system," *Neural Comput. Appl.*, vol. 30, no. 6, pp. 1991–2002, 2018, doi: 10.1007/s00521-017-3335-7.

[14] E. Kose, "Optimal Control of AVR System with Tree Seed Algorithm-Based PID Controller," *IEEE Access*, vol. 8, pp. 89457–89467, 2020, doi: 10.1109/ACCESS.2020.2993628.

[15] A. Sikander and P. Thakur, "A new control design strategy for automatic voltage regulator in power system," *ISA Trans.*, vol. 100, pp. 235–243, 2020, doi: 10.1016/j.isatra.2019.11.031.

[16] M. Micev, M. Ćalasan, and D. Oliva, "Design and robustness analysis of an Automatic Voltage Regulator system controller by using Equilibrium Optimizer algorithm," *Comput. Electr. Eng.*, vol. 89, no. March 2020, 2021, doi: 10.1016/j.compeleceng.2020.106930.

[17] M. Elsisi and M. Soliman, "Optimal design of robust resilient automatic voltage regulators," *ISA Trans.*, vol. 108, pp. 257–268, 2021, doi: 10.1016/j.isatra.2020.09.003.

[18] D. M. Sajnekar, M. L. Kolhe, S. B. Deshpande, R. M. Moharil, N. P. Patidar, and K. Ogura, "Design of PID controller for automatic voltage regulator and validation using hardware in the loop technique," *Int. J. Smart Grid Clean Energy*, vol. 7, no. 2, pp. 75–89, 2018, doi: 10.12720/sgce.7.2.75-89.

[19] N. Pachauri, "Water cycle algorithm-based PID controller for AVR," vol. 39, no. 3, pp. 551–567, 2020, doi: 10.1108/COMPEL-01-2020-0057.

[20] H. Gozde and M. C. Taplamacioglu, "Comparative performance analysis of artificial bee colony algorithm for automatic voltage regulator (AVR) system," *J. Franklin Inst.*, vol. 348, no. 8, pp. 1927–1946, 2011, doi: 10.1016/j.jfranklin.2011.05.012.

[21] M. Elsisi, "Optimal design of non-fragile PID controller," *Asian J. Control*, vol. 23, no. 2, pp. 729–738, 2021, doi: 10.1002/asjc.2248.

[22] H. Shayeghi, A. Younesi, and Y. Hashemi, "Optimal design of a robust discrete parallel FP + FI + FD controller for the Automatic Voltage Regulator system," *Int. J. Electr. Power Energy Syst.*, vol. 67, pp. 66–75, 2015, doi: 10.1016/j.ijepes.2014.11.013.

[23] N. Alawad and N. Rahman, "Tuning FPID Controller for an AVR System Using Invasive Weed Optimization Algorithm," *Jordan J. Electr. Eng.*, vol. 6, no. 1, p. 1, 2020, doi: 10.5455/jjee.204-1581071239.

[24] M. S. Ayas and E. Sahin, "FOPID controller with fractional filter for an automatic voltage regulator," *Comput. Electr. Eng.*, no. xxxx, p. 106895, 2020, doi: 10.1016/j.compeleceng.2020.106895.

[25] A. K. Bhullar, R. Kaur, and S. Sondhi, *Enhanced crow search algorithm for AVR optimization*, vol. 24, no. 16. Springer Berlin Heidelberg, 2020.

[26] P. Oziablo, D. Mozyrska, and M. Wyrwas, "Fractional-variable-order digital controller design tuned with the chaotic yellow saddle goatfish algorithm for the AVR system," *ISA Trans.*, no. xxxx, 2021, doi: 10.1016/j.isatra.2021.07.006.

[27] I. Moschos and C. Parisses, "A novel optimal PIλDND2N2 controller using coyote optimization algorithm for an AVR system," *Eng. Sci. Technol. an Int. J.*, no. xxxx, 2021, doi: 10.1016/j.jestch.2021.04.010.

[28] H. Gozde, "Robust 2DOF state-feedback PI-controller based on meta-heuristic optimization for automatic voltage regulation

system," *ISA Trans.*, vol. 98, pp. 26–36, 2020, doi: 10.1016/j.isatra.2019.08.056.

[29] I. Eke, M. Saka, H. Gozde, Y. Arya, and M. C. Taplamacioglu, "Heuristic optimization based dynamic weighted state feedback approach for 2DOF PI-controller in automatic voltage regulator," *Eng. Sci. Technol. an Int. J.*, no. xxxx, 2021, doi: 10.1016/j.jestch.2020.12.023.

[30] A. H. Mary, A. H. Miry, and M. H. Miry, "An Optimal Robust State Feedback Controller for the AVR System-Based Harris Hawks Optimization Algorithm," *Electr. Power Components Syst.*, vol. 48, no. 16–17, pp. 1684–1694, 2021, doi: 10.1080/15325008.2021.1908456.

[31] N. Aguila-Camacho and M. A. Duarte-Mermoud, "Fractional adaptive control for an automatic voltage regulator," *ISA Trans.*, vol. 52, no. 6, pp. 807–815, 2013, doi: 10.1016/j.isatra.2013.06.005.

[32] M. Elsisi, "Design of neural network predictive controller based on imperialist competitive algorithm for automatic voltage regulator," *Neural Comput. Appl.*, vol. 31, no. 9, pp. 5017–5027, 2019, doi: 10.1007/s00521-018-03995-9.

[33] M. T. Ozdemir, "A novel optimum PI controller design based on stability boundary locus supported particle swarm optimization in AVR system," *Turkish J. Electr. Eng. Comput. Sci.*, vol. 29, no. 1, pp. 291–309, 2021, doi: 10.3906/ELK-1910-81.

[34] M. Elsisi, "Improved grey wolf optimizer based on opposition and quasi learning approaches for optimization: case study autonomous vehicle including vision system," *Artif. Intell. Rev.*, no. 0123456789, 2022, doi: 10.1007/s10462-022-10137-0.

[35] T. A. Jumani *et al.*, "Jaya optimization algorithm for transient response and stability enhancement of a fractional-order PID based automatic voltage regulator system," *Alexandria Eng. J.*, vol. 59, no. 4, pp. 2429–2440, 2020, doi: 10.1016/j.aej.2020.03.005.

[36] D. İzci and S. Ekinci, "Comparative performance analysis of slime mould algorithm for efficient design of proportional–integral–derivative controller," *Electrica*, vol. 21, no. 1, pp. 151–159, 2021, doi: 10.5152/ELECTRICA.2021.20077.

[37] D. H. Wolpert and W. G. Macready, "No free lunch theorems for optimization," *IEEE Trans. Evol. Comput.*, vol. 1, no. 1, pp. 67–82, 1997, doi: 10.1109/4235.585893.

[38] A. Murdoch, R. W. Delmerico, S. Venkataraman, R. A. Lawson, J. E. Curran, and W. R. Pearson, "Excitation system protective limiters and their effect on volt/var control - design, computer modeling, and field testing," *IEEE Trans. Energy Convers.*, vol. 15, no. 4, pp. 440–450, 2000, doi: 10.1109/60.900506.

[39] S.-M. Baek, "Sensitivity Analysis Based Optimization for Linear and Nonlinear Parameters in AVR to Improve Transient Stability in Power System," *Int. J. Control Autom.*, vol. 8, no. 7, pp. 167–174, 2015, doi: 10.14257/ijca.2015.8.7.18.

[40] IEEE 421.5™-2016, *IEEE Recommended Practice for Excitation System Models for Power System Stability Studies*, vol. 2005, no. April. 2006.

[41] R. T. Sataloff, M. M. Johns, and K. M. Kost, *IEEE Guide for Identification, Testing, and Evaluation of the Dynamic Performance of Excitation Control Systems*. 2014.

[42] S. F. M. Khedr, M. E. Ammar, and M. A. M. Hassan, "Multi objective genetic algorithm controller's tuning for non-linear automatic voltage regulator," in *2013 International Conference on Control, Decision and Information Technologies (CoDIT)*, May 2013, pp. 857–863, doi: 10.1109/CoDIT.2013.6689655.

[43] M. Ćalasan, M. Micev, M. Radulović, A. F. Zobaa, H. M. Hasanien, and S. H. E. Abdel Aleem, "Optimal PID controllers for avr system considering excitation voltage limitations using hybrid equilibrium optimizer," *Machines*, vol. 9, no. 11, 2021, doi: 10.3390/machines9110265.

[44] "IEEE Recommended Practice for Excitation System Models for Power System Stability Studies," *IEEE Std 421.5-2016 (Revision IEEE Std 421.5-2005)*, pp. 1–207, 2016, doi: 10.1109/IEEESTD.2016.7553421.

[45] G. Gurrala and I. Sen, "A nonlinear voltage regulator with one tunable parameter for multimachine power systems," *IEEE Trans. Power Syst.*, vol. 26, no. 3, pp. 1186–1195, 2011, doi: 10.1109/TPWRS.2010.2069930.

[46] S. Chatterjee and V. Mukherjee, "PID controller for automatic voltage regulator using teaching-learning based optimization technique," *Int. J. Electr. Power Energy Syst.*, vol. 77, pp. 418–429, 2016, doi: 10.1016/j.ijepes.2015.11.010.

[47] G. Xu, J. Wang, and C. Chen, "Feedback stabilization for AC/DC power system with nonlinear loads," *Electr. Power Syst. Res.*, vol. 74, no. 2, pp. 247–255, 2005, doi: 10.1016/j.epsr.2004.11.003.

[48] P. M. Patil and D. S. K. Patil, "Automatic Voltage Regulator," *Int. Conf. Emerg. Trends Inf. Technol. Eng. ic-ETITE 2020*, pp. 1–5, 2020, doi: 10.1109/ic-ETITE47903.2020.476.

[49] S. Duman, N. Yörükeren, and I. H. Altaş, "Gravitational search algorithm for determining controller parameters in an automatic voltage regulator system," *Turkish J. Electr. Eng. Comput. Sci.*, vol. 24, no. 4, pp. 2387–2400, 2016, doi: 10.3906/elk-1404-14.

[50] Z. Bingul and O. Karahan, "A novel performance criterion approach to optimum design of PID controller using cuckoo search algorithm for AVR system," *J. Franklin Inst.*, vol. 355, no. 13, pp. 5534–5559, 2018, doi: 10.1016/j.jfranklin.2018.05.056.

[51] L. F. P. Silva, V. J. S. Leite, E. B. Castelan, M. Klug, and K. Guelton, "Local stabilization of nonlinear discrete-time systems with time-varying delay in the states and saturating actuators," *Inf. Sci. (Ny).*, vol. 518, pp. 272–285, 2020, doi: 10.1016/j.ins.2020.01.029.

[52] M. Furat and I. Eker, "Chattering-eliminated adaptive sliding-mode control: An experimental comparison study," *Turkish J. Electr. Eng. Comput. Sci.*, vol. 24, no. 2, pp. 605–620, 2016, doi: 10.3906/elk-1309-137.

[53] M. Furat and I. Eker, "Second-order integral sliding-mode control with experimental application," *ISA Trans.*, vol. 53, no. 5, pp. 1661–1669, 2014, doi: 10.1016/j.isatra.2014.05.030.

[54] A. Levant, "Principles of 2-sliding mode design," *Automatica*, vol. 43, no. 4, pp. 576–586, 2007, doi: 10.1016/j.automatica.2006.10.008.

[55] K. Zeb, T. Davi, C. Busarello, S. U. Islam, and W. Uddin, "Design of Super Twisting Sliding Mode Controller for a Three-Phase Grid-connected Photovoltaic System under Normal and Abnormal Conditions," *Energies*, vol. 13, no. 3773, p. 20, 2020.

[56] F. U. Rehman, M. R. Mufti, S. U. Din, H. Afzal, M. I. Qureshi, and D. M. Khan, "Adaptive smooth super-twisting sliding mode control of nonlinear systems with unmatched uncertainty," *IEEE Access*, vol. 8, pp. 177932–177940, 2020, doi: 10.1109/ACCESS.2020.3027194.

[57] N. M. H. Norsahperi and K. A. Danapalasingam, "An improved optimal integral sliding mode control for uncertain robotic manipulators with reduced tracking error, chattering, and energy consumption," *Mech. Syst. Signal Process.*, vol. 142, p. 106747, 2020, doi: 10.1016/j.ymssp.2020.106747.

[58] Y. Huangfu *et al.*, "Control of MagLev System Using Supertwisting and Integral Backstepping Sliding Mode Algorithm," *IEEE Access*, vol. 8, no. 4, pp. 51352–51362, 2020, doi: 10.1109/ACCESS.2020.2980687.

[59] V. I. Utkin, "Variable Structure Systems with Sliding Modes," *IEEE Trans. Automat. Contr.*, vol. AC-22, no. 2, pp. 212–222, 1977.

[60] Z. Liu and Q. Wang, "Hybrid control with sliding-mode plus self-tuning PI for electrical machines," *J. Electr. Eng.*, vol. 59, no. 3, pp. 113–121, 2008.

[61] M. Elsisi and H. Abdelfattah, "New design of variable structure control based on lightning search algorithm for nuclear reactor power system considering load-following operation," *Nucl. Eng. Technol.*, vol. 52, no. 3, pp. 544–551, 2020, doi: 10.1016/j.net.2019.08.003.

[62] A. Raza, F. M. Malik, N. Mazhar, H. Ullah, and R. Khan, "Finite-Time Trajectory Tracking Control of Output-Constrained Uncertain Quadrotor," *IEEE Access*, vol. 8, pp. 215603–215612, 2020, doi: 10.1109/ACCESS.2020.3041262.

[63] A. Kanchanaharuthai and E. Mujjalinvimut, "A composite nonlinear controller for higher-order models of synchronous generators under external disturbances," *Int. J. Innov. Comput.*

Inf. Control, vol. 15, no. 2, pp. 465–478, 2019, doi: 10.24507/ijicic.15.02.465.

[64] I. Eker, "Second-order sliding mode control with experimental application," *ISA Trans.*, vol. 49, no. 3, pp. 394–405, 2010, doi: 10.1016/j.isatra.2010.03.010.

[65] M. Furat and İ. Eker, "Experimental Evaluation of Sliding-Mode Control Techniques," *Çukurova Univ. J. Fac. Eng. Archit.*, vol. 27, no. June, pp. 23–37, 2012.

[66] O. Camacho and C. A. Smith, "Sliding mode control: An approach to regulate nonlinear chemical processes," *ISA Trans.*, vol. 39, no. 2, pp. 205–218, 2000, doi: 10.1016/s0019-0578(99)00043-9.

[67] I. Eker, "Second-Order Sliding Mode Control with PID Sliding Surface and Experimental Application to an Electromechanical Plant," *Arab. J. Sci. Eng.*, vol. 45, no. 1, pp. 109–118, 2006, doi: 10.1007/s13369-012-0290-6.

[68] C. J. Fallaha, M. Saad, H. Y. Kanaan, and K. Al-Haddad, "Sliding-mode robot control with exponential reaching law," *IEEE Trans. Ind. Electron.*, vol. 58, no. 2, pp. 600–610, 2011, doi: 10.1109/TIE.2010.2045995.

[69] I. Kaya, "Sliding-mode control of stable processes," *Ind. Eng. Chem. Res.*, vol. 46, no. 2, pp. 571–578, 2007, doi: 10.1021/ie0607806.

[70] I. Eker and Ş. A. Akinal, "Sliding mode control with integral augmented sliding surface: Design and experimental application to an electromechanical system," *Electr. Eng.*, vol. 90, no. 3, pp. 189–197, 2008, doi: 10.1007/s00202-007-0073-3.

[71] I. Fister, X. S. Yang, J. Brest, and D. Fister, "A brief review of nature-inspired algorithms for optimization," *Elektroteh. Vestnik/Electrotechnical Rev.*, vol. 80, no. 3, pp. 116–122, 2013.

[72] J. Kennedy and R. Eberhart, "Particle Swarm Optimization," *Part. Swarm Optim.*, pp. 1942–1948, 2010, doi: 10.1002/9780470612163.

[73] G. Gidemen and M. Furat, "Parçacık Değiştirmeli PSO Algoritması," pp. 1–6, 2017, doi: doi.org/10.1109/IDAP.2017.8090259.

[74] D. L. Cushman, "A Particle Swarm Approach to Constrained Optimization Informed by ' Global Worst ,'" *East*, 2007.

[75] H. Liu, G. Xu, G. Ding, and Y. Sun, "Human Behavior-Based Particle Swarm Optimization," vol. 2014, no. 4, 2014.

[76] S. R. Desai and R. Prasad, "A new approach to order reduction using stability equation and big bang big crunch optimization," *Syst. Sci. Control Eng.*, vol. 1, no. 1, pp. 20–27, 2013, doi: 10.1080/21642583.2013.804463.

[77] M. Garg, "Model order reduction and approximation analysis for control system design," *4th IEEE Int. Conf. Signal Process. Comput. Control. ISPCC 2017*, vol. 2017-Janua, no. 1, pp. 473–476, 2017, doi: 10.1109/ISPCC.2017.8269725.

[78] M. Furat and I. Eker, "Computer-aided experimental modeling of a real system using graphical analysis of a step response data," *Comput. Appl. Eng. Educ.*, vol. 22, no. 4, pp. 571–582, 2014, doi: 10.1002/cae.20482.

[79] W. N. Chen *et al.*, "Particle swarm optimization with an aging leader and challengers," *IEEE Trans. Evol. Comput.*, vol. 17, no. 2, pp. 241–258, 2013, doi: 10.1109/TEVC.2011.2173577.

MURAT FURAT was born in Kilis, in TURKEY, in 1977. He received a B.S. degree Electrical-Electronics Engineering Department from Gaziantep University, an M.S. degree in Electronics Engineering Department from Mustafa Kemal University, and a Ph.D. degree in Electronics Engineering Department from Çukurova University. From 2002 to 2014, he was a research assistant. Since 2014, he has been an Assistant Professor at İskenderun Technical University.

His research interests are sliding mode control, optimization of controllers, the internet of things, and other areas closely related to the industry according to the professions of his postgraduate students.

GÖKÇEN GİDEMEN CÜCÜ was born in İskenderun, HATAY, TURKEY in 1992. She graduated in Electrical-Electronics Engineering Depertment from Erciyes University, in Kayseri, in 2013 and studied M.S. on Tuning of PID Parameters with Renewed Particle Swarm Optimization from İskenderun Technical University, in 2018. Since 2014, she has been an Instrument and Control Engineer in the Instrument and Control Department of Atlas Energy Thermal Power Plant in HATAY.